

Ceramics from Self-Sustained Reactions: Recent Advances

A.S. Mukasyan^{a*}, D.O. Moskovskikh^b, A.A. Nepapushev^b, J.M. Pauls^a, S.I. Roslyakov^b

^a Department of Chemical and Biomolecular Engineering, University of Notre Dame, Notre Dame, Indiana, 46556, USA

^b Center of Functional Nano-Ceramics, National University of Science and Technology "MISIS", Moscow, 119049, Russia

* Corresponding author: amoukasi@nd.edu

Keywords: combustion synthesis, solution combustion synthesis, ceramics, spark plasma sintering, mechanical activation, shockwave processing

Abstract

Specific applications of self-sustained reactions to fabricate advanced ceramics, along with details such as synthesis conditions, mechanism of microstructure formation, and material properties, are overviewed. The latest achievements in the field include analysis of three such synthetic routes: reactive spark plasma sintering, combustion synthesis with mechanical stimulation, and solution combustion synthesis. Examples of fabrication of high-temperature nanostructured ceramics and composites, as well as non-equilibrium ceramic phases are also discussed.

Table of Content

1. Introduction	2
2. Combustion synthesis routes	5
2.1. CS and high energy ball milling.....	5
2.2. CS and spark plasma sintering.....	8
2.3. CS and shockwave processing.....	10
2.4. Solution combustion synthesis.....	13
3. Combustion Synthesis of Ceramics	16
3.1. Ceramics by combination of CS and HEBM: Morphology control.....	16
3.2. CS and SPS: Rapid synthesis of bulk high-temperature ceramics.....	19
3.3. Shock-induced synthesis of ceramics containing metastable c-BN phase.....	24
3.4. Solution combustion synthesis of a metastable metal nitride.....	27
4. CS: Future directions	29
References	31

1. Introduction

The most general definition of combustion phenomenon implies the chemical reaction that self-propagates along the media, localizing in relatively thin combustion zone. The conventional examples for such processes include burning of coal and candles, forest fires, and gasoline combustion in engines. In these examples, the presence of gas phase oxygen is critical and the desired combustion products are heat, light, and power. This review covers a different type of combustion paradigm that is those combustion processes that may occur without oxygen with the primary aim of producing valuable solid-state materials. Two such types of combustion processes are considered in this review. The first is solid-state reaction in a powder-based media, while the second is combustion of reactive solutions.

In the late 1960s a group of researchers from the Institute of Chemical Physics, part of the USSR Academy of Sciences, headed by Alexander Merzhanov, searched for self-sustained combustion reactions of propellants that might burn without producing a gas flame. During this work, the scientists discovered a new phenomenon of “reaction wave localization for solid state reactions” [1] or in modern terms the *solid flame* [2,3]. To explain this phenomenon let us consider the tantalum (Ta) – carbon (C) reactive system. Thermodynamic analysis reveals that this system is highly exothermic, which means that, if reaction between these precursors is initiated, a large amount of heat (2120 cal/cc) may be released, and for adiabatic conditions the combustion temperature may reach as high as 2470 °C. However, the Ta-C equilibrium phase diagram indicates that the melting points (m.p.) of the precursors are 3020 °C for Ta and 3800 °C for carbon, with a eutectic point of 2843 °C [4]. All these temperatures are well above the adiabatic combustion temperature, which implies that the combustion process should proceed without the presence of any liquid or gaseous species, but instead should progress solely due to solid-state mass transport mechanisms. Therefore, observation of self-sustained localized reaction in this system can be considered as evidence of a solid flame.

Examination of the more than fifty years of fundamental studies of solid flame phenomenon is very enlightening, but it is outside the scope of this work and can be found in recent publications [5,6]. For production of ceramics, it is more relevant that the only combustion product in the Ta-C system is the valuable ultra-high temperature ceramic, tantalum carbide (m.p. 3985 °C). The concept of using gasless combustion reactions in heterogeneous powder mixtures to produce materials was broadened to thousands of reactive systems. Currently this approach, known as conventional combustion synthesis (CS), allows fabrication of almost any type of advanced ceramics [1,7,8]. The unique parameters of this approach includes: (i) high temperatures (2000 – 4000 °C), which in many cases exceed those that can be achieved in furnaces; (ii) extremely high heating rates (up to 10^6 °C/s) within the combustion front, which may lead to the formation of non-equilibrium phases; (iii) short synthesis time (10^{-6} – 10 s); (iv) essentially zero energy consumption; (v) simple technological equipment; and (vi) in many cases, easy scalability [1,3,9]. The often-discussed disadvantages are as follows: (i) the controllability of the combustion process, where all parameters are closely correlated; (ii) structural uniformity of the produced materials; and (iii) process safety [3]. In this review we demonstrate the strong aspects of the conventional CS process and discuss routes to overcome the drawbacks.

In the middle of 1980s scientists from India, P. Ravindranathan, and K. Patil, discovered that the paradigm of “self-sustained reaction for materials synthesis” can also be applied for reactive aqueous solutions [10,11]. These solutions involve oxidizers, typically metal nitrate hydrates, and fuels (urea, glycine, citric acid, etc.). Both the oxidizer and the fuel are often solids at room temperature but have high solubility in water. Thoroughly mixed solutions of fuel and oxidizer are exothermic, with adiabatic combustion temperatures in the range 1000 – 2000 °C. Therefore, while all the advantages of materials synthesis mentioned for heterogeneous conventional CS are applied here, solution combustion synthesis (SCS) has its own specific advantages. First, in this case, the reactants are mixed on the molecular level, thus by clever control of the process it is easy to fabricate nano-sized materials. Second, typically a large amount of

gaseous sub-products form during SCS, which hinders sintering of the solid product and leads to synthesis of high surface area powders. Finally, high combustion temperatures permit one-step synthesis of crystalline materials, thus avoiding additional post-synthesis high-temperature treatment (calcination) of the product. The general concerns for SCS are as follows: (i) it is difficult to produce separate particles with a narrow size distribution; (ii) primarily oxides ceramics can be fabricated. Indeed, during the last decade, thousands of different oxides, including binary oxides, ternary oxides, and multi-element perovskites, have been produced by SCS [11,12]. However, the range of SCS products has recently been expanded to include pure metals, alloys, intermetallics and metal nitrides ceramics [12–14]. The typical morphology of SCS products consists of high surface area porous sponge-like agglomerates and only recently developed routes permit synthesis of nano-sized particles with a narrow particle size distribution [15]. In this review, we discuss recent breakthroughs in the field of SCS, focusing on the controllability of the process, which can be achieved based on investigation of the reaction mechanisms taking place within the combustion wave.

It should be noted that both CS approaches, i.e. heterogeneous conventional SC and homogeneous SCS, can be accomplished in two different reaction modes. The self-propagating high-temperature synthesis (SHS) mode involves local preheating of the reaction media, followed by reaction propagation along this media in the form of a high temperature combustion front. The second mode, volume combustion synthesis (VCS), implies uniform preheating of the reactant material to the so-called ignition temperature, at which reaction starts essentially uniformly across the entire volume.

The goal of this review is to summarize and discuss the specifics for CS of ceramics, including synthesis conditions, mechanism of microstructure formation, as well as material properties. Special attention is paid to the latest achievements in the field, including analysis of such novel synthetic routes as reactive spark plasma sintering, combustion synthesis with mechanical stimulation, CS of nanostructured ceramics and composites, as well as fabrication of non-

equilibrium phases. In section 2 we overview recently developed routes for synthesis of ceramics, focusing on the hybrid approaches that involve a combination of different advanced synthesis methods with CS. In section 3 using examples of ceramics fabricated in our laboratories, we illustrate the capabilities of these approaches, showing synthesis of sub-micron powders, dense bulk nanostructured ceramics, and non-equilibrium phases. In section 4 we briefly discuss future directions of the CS field.

2. Combustion synthesis routes

2.1. CS and high energy ball milling

Treatment of powder mixtures in different types of mills is a well-known technique in powder metallurgy [16]. For example, as developed in the late 1960s, mechanical alloying (MA) process is one of the effective methods for production of equilibrium and non-equilibrium alloys. In general, MA involves high-energy milling devices, including attritor, vibrational, and ball mills. However, conventional MA usually involves long-term (tens of hours) treatment and cannot be applied for energetic systems.

A hybrid approach that combines short-term high-energy ball milling (HEBM) of reactive powder mixtures with combustion synthesis is also widely used to produce different materials [1,17–20]. Initially this approach was suggested as an activation tool for low exothermic CS mixtures [18,20]. Indeed, many important reactions, including B+C, B+TiN and Si+C, which lead to the fabrication of B₄C, BN-TiB₂, and SiC ceramics, have relatively low enthalpy of product formation. and, thus, low adiabatic combustion temperatures. The temperature associated diffusion limitations prevent these reactions from proceeding in a self-sustained manner when prepared as a conventional mixture of reactant powders. However, CS in these systems can be accomplished by using different so-called activation methods, such as preliminary preheating [21], introduction of functional additives [22], or by preliminary mechanical treatment [23]. It was demonstrated that optimized HEBM of such powder mixtures results in significant enhancement of their reactivity, which leads to the realization of the steady-state self-sustained reaction mode

[17,20,24]. Unlike conventional MA, the idea of short-term HEBM is to “activate” the reaction without any chemical interaction between the components of the mixture. Therefore, the process is interrupted (arrested) at some critical time in order to obtain a reactive media with increased reactivity prior to the occurrence of chemical reaction. The duration of short-term HEBM depends on the system and the milling conditions. For example, it is 3 min for the Ti-C system [25] and 45 min for the B-TiN system [26].

Several mechanisms have been suggested to explain the effect of reaction activation by short-term HEBM (see discussion in [27]). In our opinion, two factors play the most important role. First, there is a significant increase in contact surface area between the reactants. Initially, powder-based reactants have only point contacts. Due to severe plastic deformation of the reactive powder under the influence of the milling bodies inside the milling container, more ductile powder particles are repeatedly flattened and deformed, while brittle powders break and decrease in size. Continued impact of the bodies leads to the cold-welding of particles producing composite particles, which contain both precursors (Fig. 1a).

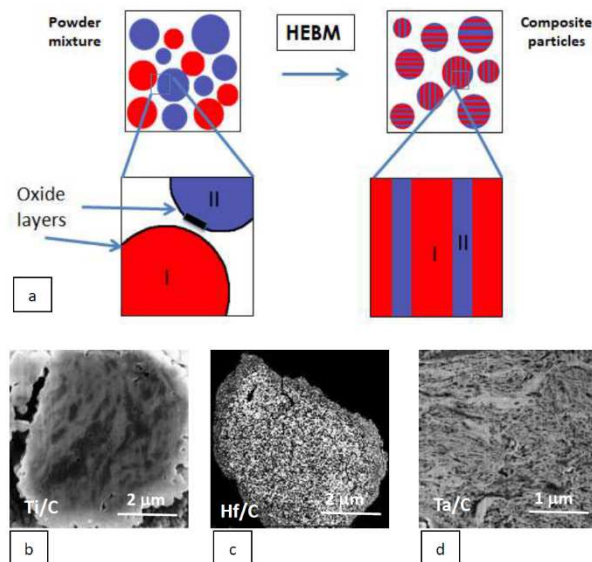


Fig. 1. (a) Schematics for formation of composite particle during HEBM; Cross sections of the mechanically-induced particles in (b) Ti-C; (c) Hf-C; and (d) Ta-C systems.

Increasing the duration of mechanical treatment, which typically takes place in an inert gas atmosphere, leads to the formation of fresh oxygen-free contact surfaces. The second factor in

increased reactivity is related to the simultaneous decrease of the characteristic diffusion scales (size of the particulates) to the nano-level. Figures 1 b-d shows typical cross sections of mechanically-induced composite particles in different metal-carbon (Ti/C; Hf/C; Ta/C) systems. It can be seen that the characteristic sizes of the precursors range from 10 to 100 nm. Both the increased surface area contact and reduced characteristic size promote solid-state diffusivity and are responsible for the increased reactivity of treated mixtures allowing implementation of CS even for weakly exothermic mixtures.

Recently, it was realized that a similar approach can also be applied for highly exothermic systems. While not needed to enhance reactivity, mechanical treatment can be used to control the microstructure of the fabricated ceramics [24]. Controllability of the microstructure of the materials produced by CS is a well-recognized issue [1,3] . Indeed, because of the rapid self-sustained nature and extremely high-temperatures, which typically exceed melting points of the precursors, it is difficult to control the structural transformation processes in the combustion front. However it was demonstrated that if the diffusion scales in the composite reactive particles are below some critical values, the reaction occurs so rapidly, that melting does not significantly influence the structural transformations of the media, hence the morphology of the produced powders essentially mimic that of the initial composite particles [1,28].

In the suggested approach, the initial reactive medium structure plays one of the major roles in the structural formation of CS materials. HEBM has been proven to be a powerful tool to control the morphology and structure of the composite reactive particles. For example, it was shown that by using a planetary ball mill and changing the K parameter, the ratio between the rotation speeds of the grinding vial and the sun wheel, it is possible to achieve different types of ball movement inside the milling vial: cascading, cataracting, and centrifugal [28]. These different regimes significantly change the structure and morphology of the produced composite reactive particles and, as such, also their reactive properties. Therefore, by the optimization of HEBM parameters one can control the morphology of milled powders and thus the powder structure after CS. The

approach to control morphology of the ceramic powders produced by CS is discussed in detail in Section 3.1.

2.2. *CS and spark plasma sintering*

In recent years, several novel methods have been developed for the consolidation of powder materials, including sub-micron and nano-ceramics, which make it possible to control the grain growth process and reduce the sintering time to several minutes [29]. One of these methods is spark plasma sintering (SPS) (cf. [30–34]). The main idea of SPS involves the passage of large (1000-5000 Amps) pulses of an electric current through the media to be consolidated, which should lead to the formation of plasma at the spot-like inter-particle contacts, thus facilitating mass transfer and sintering. It is interesting that this concept was conceived when one of the inventors Dr. Z. Munir was investigating the combustion of low exothermal CS systems and suggested electrical current as a reaction “activation” tool [35–38].

Recently, the combination of SPS and CS was revisited at a qualitatively new level due to advances in the currently available SPS devices. In the case of reactive spark plasma sintering (RSPS), in addition to the obvious SPS effects of high temperature, high heating rates, and high axial pressure, the joule heating promotes the initiation of self-sustained reactions in the consolidated media, which further accelerates sintering to obtain bulk ceramics (cf. [39–45]). The typical scheme of the RSPS device is shown in Fig. 2a. The reactive mixture of powders (e.g. Si+C [43] or B₄C-(Ti₃SiC₂+Si) [45]) or reactive foils (e.g. Mo foils and Si wafers in a Mo–Si–Mo multilayer assembly [30]) is placed into a cylindrical graphite die. A graphite paper was positioned between the sample and the die to protect the surface of the die from chemical interaction with the reactive media. The important issue for RSPS is the time history of pressure application. To avoid damage to the die at the moment of reaction initiation, it is recommended to initially apply a relatively low pressure and increase it just after reaction begins.

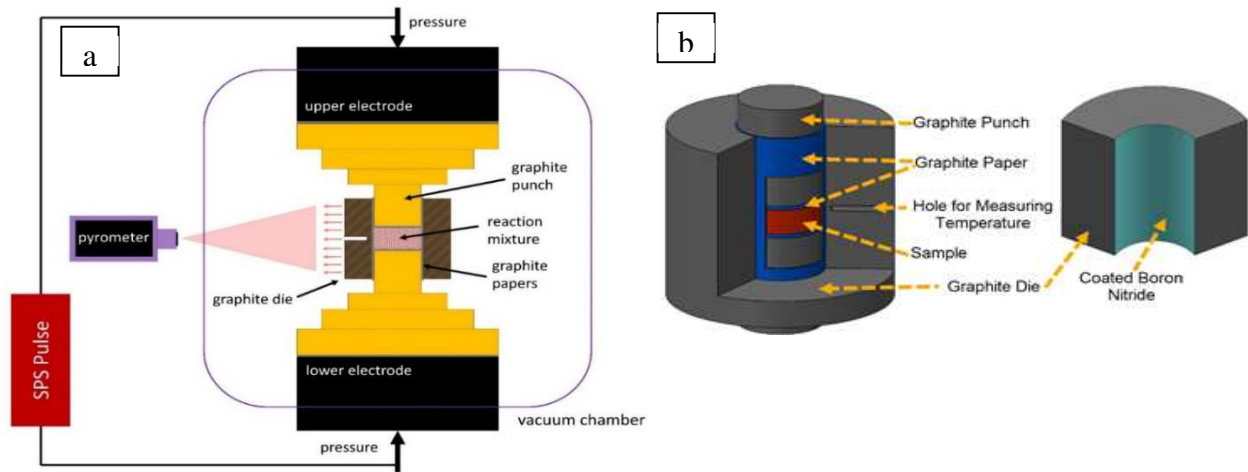


Fig. 2. Schematics of: (a) SPS/RSPS device with reaction mixture and (b) the FSPS scheme.

Another SPS-based approach is flash spark plasma sintering (FSPS) [46–50]. The general concept is to preheat pre-compacted powder specimens to a critical temperature before applying any voltage to the powder volume and allowing the electrode-punches of the SPS device setup to contact the specimens, and pass electric current through them under elevated temperatures. This runaway process, with heating rates of up to 10 000 C/min, permits ultra-fast (seconds) consolidation of the ceramics produced. The possible mechanisms for such phenomenon are discussed in [48] and include electrical breakdown and formation of defects.

Several methods for consolidation during FSPS have been suggested in the literature. In most of them press dies cannot be used, which prevents application of pressure during sintering [48]. Additionally, such schemes do not permit sintering of initially electrically non-conductive materials [47]. Therefore, for initially non-conductive mixtures (e.g. $\text{Al}_2\text{O}_3\text{-SiC}$), we used the configuration suggested by Manière et al. [48] that allows the application of pressure during FSPS treatment and thus accelerates the sintering process. In this scheme the inner surface of the die is coated by an electrically insulating boron nitride (BN) layer (see Fig. 2b) and the effectiveness of the insulation between the graphite die and the punches was verified before and after sintering. At low temperatures under FSPS condition, the non-conductive sample is electrically insulated, which causes the current to pass primarily through the thin graphite paper. At this stage, the current and

voltage of the system rapidly rise, which leads to an extremely rapid increase in temperature (more than 100 °C/s). The system pressure may be varied up to 90 MPa. However, sample resistivity decreases with temperature and, at some point, it becomes sufficiently conductive and the “flash” phenomena occurs. At this stage, the rapid densification of the powder compact leads to a sharp positive displacement over a very short time-period (10-30 s). Similarly to SPS/RSPS conditions, one can envision the use of a reactive flash spark plasma sintering (RFSPS) scheme, where reactive media can be consolidated with simultaneous transformation of initial precursors to the desired ceramic products. Results from the application RSPS to Si-C and B-C systems are discussed in Section 3.2.

2.3. *CS and shockwave processing*

The combined application of CS and a shockwave is another promising hybrid route to produce ceramics. The shockwave may play a triple role in material synthesis by providing conditions for: (i) consolidation; (ii) reaction initiation; and (iii) the synthesis of phases that can only be formed at high pressure. The pressure in a typical shockwave experiment ranges from 3 to 80 GPa, which is sufficient to consolidate any powder media to near maximum relative density, as well as to induce different phase transformations [51–54].

Specifically, two methodologically different routes for CS of ceramics in combination with application of a shockwave have been suggested. The first involves thermal initiation of the combustion reaction followed by an applied shock to the reacted media. Two possible schemes for high-speed loading by shock waves of the media after reaction initiation are presented in Fig. 3a: one (left) provides axial and the other (right) radial densification [55]. In both cases the sample (1), preliminarily compacted from a reactive powder mixture of the desired composition, is ignited with a hot metal wire (2) at the bottom of metal container (3), and after an optimized delay time after ignition, the explosives (4) are detonated by an electro-detonator (5) mounted on the top of the set-up. In one case (Fig. 3a, left) the material is compacted by a sliding detonation wave front through a thin-walled cylindrical container (3). In the other (Fig. 3a, right), a detonation wave

propagating normal to the axis is used for acceleration of the metal plate (6). The dynamic axial densification method has been used to synthesize dense ultra-high temperature ceramics including TiC, TiB₂, and HfC [55–59]. The radial shock-wave densification technique was applied to produce several materials, including the dense high-temperature ceramic superconductor YBa₂Cu₃O_{7-x} [59].

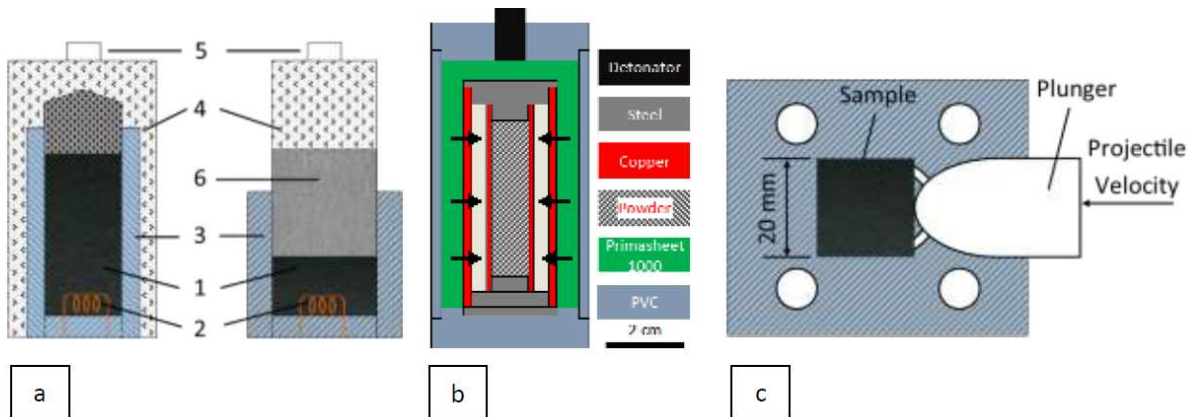


Fig. 3. Schematics of experimental set-ups for combination of CS and shock wave.

The second route is based on the observed fundamental phenomenon that reaction in CS heterogeneous mixture may occur directly as a result of application of a shock wave (cf. [60–62]). The diagram shown in Fig. 3b, is similar to Fig. 3a left: reactive powder mixture is loaded into a thin metal (typically copper) recovery capsule, which is closed from both sides by stainless-steel caps. The capsule was selected to sustain the high pressure from the shock wave for a longer duration as compared to direct contact with an explosive [63]. The mixture is shocked by an explosive (such as PrimaSheet 1000) to drive the outer shell at high velocities into the central tube that contains the powder. This approach, which has been termed shock-induced reaction synthesis (SRS), was developed during the 1990s [62,64–66] and a variety of dense silicides (e.g., MoSi₂, NbSi₂, Ti₅Si₃, TiSi₂) and aluminides (NiAl, NiAl₃) have been synthesized using this method.

Reactive CS mixtures have also been used for rapid preheating (as a chemical oven) of the media to be shocked. In this case the reactive CS mixture and an ampoule with the target materials, are placed into a tube made from refractory metal. Following initiation of the reactive CS mixture,

the target materials are heated with subsequent ampoule compaction by the shock wave. This configuration can be useful for cases, such as the synthesis of diamond, which require both high temperatures and high pressure.

The other configuration (Fig. 3c) is known as the Asay shear impact experiment [67]. Briefly, the sample for the experiments is produced through cold-pressing the reactive powders into a rectangular solid with dimensions 2 cm x 2 cm x 0.2 cm. The moving piston impacts a plunger, which presses against the narrow face of the sample, creating shear. The geometry of the plunger surface that impinges on the sample can be adjusted to control and determine the applied strain field. A light-bore gas gun is used to accelerate the piston. Typically, the piston velocities range from 100 ms⁻¹ to 1500 ms⁻¹, providing muzzle energies from 0.1 to 25 kJ. The rectangular window permits observation of the reaction phenomenon.

It was shown that when the projectile energy exceeds some threshold value the reaction takes place in a thin layer of the sample during the impact, and after an approximately 1 ms delay, a combustion front propagates along the compacted media in a manner similar to that observed for thermal initiation of the reaction. This is the so-called shock-initiated reaction mode. However, further increases of the projectile velocity lead to an increased thickness of the layer reacted during impact, and at some critical point, the thickness becomes equal to the length of the sample. In this case, the characteristic reaction time is on the order of microseconds. This reaction mode can be considered as mechanically-induced thermal explosion mode [68]. Recent results using the shock-induced reaction synthesis approach to fabricate ceramic materials that involve non-equilibrium phases will be discussed in Section 3.3.

2.4. Solution combustion synthesis

Self-sustained reactions in solutions or sol-gels are an exciting phenomenon that has been widely used for synthesis of ceramics [8,12,69]. All solution combustion synthesis (SCS) routes include preparation of homogeneous solutions of an oxidizer (typically metal nitrates) and organic fuels (glycine, urea, citric acid, etc.) in a solvent (water, alcohols, etc.). The specifics of each SCS

route depends on the scheme for the reaction initiation, as well as on the method for preliminary treatment of the reactive solution.

Like the conventional heterogeneous CS, the combustion process can be accomplished in two different modes. In the most common case, the solution is placed into a preheated muffle furnace or a hot plate with temperature in the range 300–700 °C [70]. After evaporation of the solvent, a viscous gel-like matter forms, followed by the initiation of combustion reaction essentially along the whole volume of the media with rapid evolution of a significant amount of gases and formation of the solid products with the desired phase composition. This is the volume solution combustion synthesis (VSCS) combustion mode (Fig. 4a). Alternatively, a smaller volume of the solution may be locally heated by a hot metal wire to initiate the exothermic reaction. After the initiation, the reaction self-propagates along the rest of the volume in the form of a high-temperature combustion wave (Fig. 4b). This SCS mode resembles the SHS mode observed in solids [8]. It is worth noting that the SHS mode is a more controllable process, as compared to VSCS mode and allows synthesis of ceramics with more uniform microstructure and properties [13,71].

Taking into account the fact that the initial reactive solution has low viscosity, several SCS modifications have been suggested. These routes involve impregnation of the solution into a variety of porous solid support (layer) followed by initiation of self-sustain reactions in such composite media. The layer may be chemically inert (such as with high surface area porous oxides), known as impregnated SCS in porous inert media [72–75], or reactive (cellulose), known as SCS in an active layer [76,77]. The former route is typically used to fabricate nanostructured

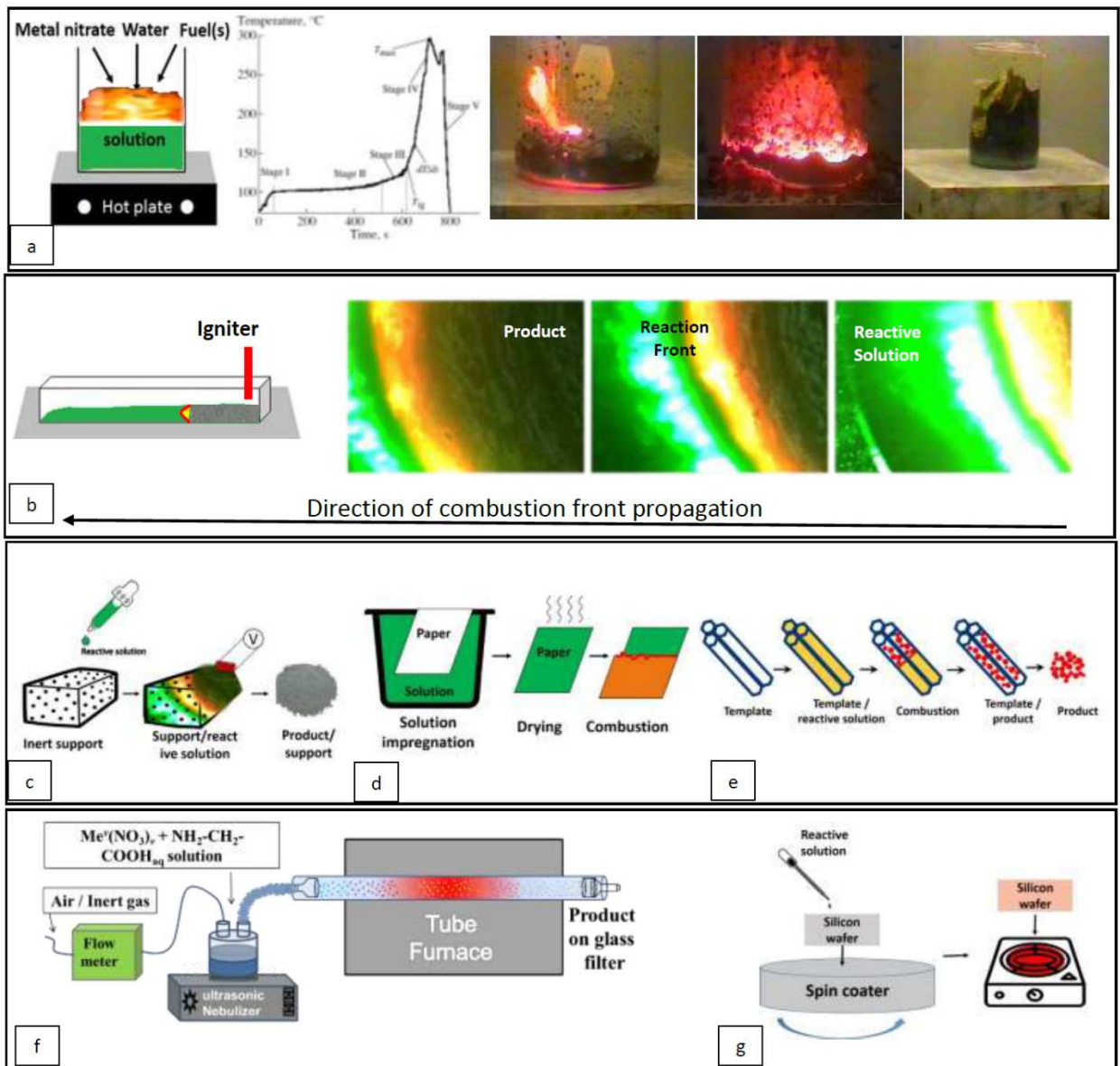


Fig. 4. Schematics of different SCS routes: (a) VSCS and (b) SHS modes; (c) SCS in an inert media, (d) SCS in an active layer, (e) template SCS, (f) SSCS and (g) SCS of thin films.

supported ceramic catalysts with a high specific surface (Fig. 4c). The latter approach (Fig. 4d) is used to synthesize ceramic powders using low exothermic systems for which combustion of the active layer facilitates the propagation of the reaction front [71]. Both cases consist of similar steps: preparation of the desired reactive solution, selection of the appropriate support, solution impregnation onto the porous support, drying, and, finally, initiation of a self-sustaining combustion reaction. These routes are also suitable for development of continuous powder production technologies (see [71] for details).

Another approach that is also related to the impregnation technique is called template assisted solution combustion synthesis (or template SCS) [15,78]. In this case the role of the solid media is played by a porous template with a desired pore diameter that allows control over the size and shape of the synthesized particles. For example, spherical nanoparticles form inside the nanotubes with sizes equal to the diameter of these tubes (Fig. 4e). After synthesis, the porous template media is removed (dissolved), and nanoparticles with a narrow size distribution are extracted. This suggested approach enables the production of uniform nanostructures such as non-agglomerated nanoparticles, nanotubes, nanorods, two-dimensional crystals, and ordered mesoporous solids [15,78,79].

Heating method in all the above approaches also have significant impact on the properties of the resulting materials. For example, microwave heating fundamentally differs from conventional thermal heating processes [80,81]. In this case, the heat is directly generated in the materials volume by the interaction of the electromagnetic field with electric and magnetic dipoles in the heated media. Thus, the interaction of the applied alternating electromagnetic field with the reactive aqueous solution is uniquely related to the electro-physical properties of the materials.

Many features of SC are present in a liquid aerosol flame synthesis [82,83]. One of the varieties is spray solution combustion synthesis (SSCS) [84–86]. The synthesis of hollow spherical particles (ceramics, metals, cermet etc.) occurs in the flux of inert (or reactive) gas solely due to the reaction between fuel and oxidizer, which are the precursors for the sprayed solution (Fig. 4f). The unique characteristic of spray-based combustion method is that it allows the fabrication of spherical particles with relatively narrow size distributions, which is difficult to achieve by other SCS approaches. It is also notable that SSCS fabricated hollow particles possess exceptionally high sinterability due to the extremely active nanostructured surface of the spheres [86].

Most recently, a novel SCS-based method has been reported for the production of high-quality thin films for electronic devices and solar cell applications [87]. This technique involves deposition of a prepared reactive solution onto a hard (silicon wafer) or soft (flexible polymer)

substrate using either spin coating or spraying techniques (Fig. 4g). Combustion of the thin precursor layer produces a uniform high-quality film for different electro-chemical applications [12].

Using the metal nitrate and oxygen-containing fuels allows CS of a wide variety of oxides, including complex perovskites [12,69,88]. The goal of many current research efforts is to widen the list of the compounds, which can be fabricated by the SCS approach. Various pure metals and alloys have been successfully synthesized [13,89–91], and, recently, the synthesis of a metal nitride was reported [14]. In Section 3.4, the fundamental aspects of the formation of a non-equilibrium iron nitride phase in the combustion wave are discussed in detail. This breakthrough finding opens new venues for application of the SCS method for production of unique ceramic materials.

3. Combustion Synthesis of Ceramics

3.1. Ceramics by combination of CS and HEBM: Morphology control

The microstructure of CS-powders may significantly change during CS, as a result of melting of the precursors. Investigation of the fundamental mechanisms of structure transformation under CS conditions is required to resolve the essential issue of controlling the morphology of CS-powders. This is a challenging task because of the high temperatures (1500-3000 K), short reaction times (~ms) and small structural scales (10^{-3} -100 μm) inherent to the CS process [1–3]. However, an alternative route exists and is based on the concept that the microstructure of certain specially prepared initial reactive powders does not undergo changes within the reaction front. In this case, by controlling the microstructure of the initial mixture, one can control the morphology of the synthesized ceramic powders. This novel approach is based on the use of HEBM to prepare reactive powders.

As discussed in section 2.1, by varying the HEBM regimes one can control the microstructure of the processed material [16,28]. Under certain milling conditions reactive nanostructured composite particles can be fabricated, which contain precursors mixed at the level

of tens to hundreds of nanometers (Fig. 1 b-d). It has been demonstrated that by producing such short diffusion lengths, the morphology of the particles remains essentially unchanged after CS even at temperatures that exceed the melting points of the precursors [28].

The Ti - C system is highly exothermic ($\text{Ti} + \text{C} = \text{TiC} + 230 \text{ kJ/mol}$) with an adiabatic combustion temperature of $\sim 3000 \text{ }^\circ\text{C}$ [2]. The reaction mechanism in conventionally prepared Ti+C mixtures involves the melting of Ti, C dissolution in the melt, followed by crystallization of TiC grains [92]. One should precisely control the dissolution-crystallization kinetics to fabricate powders with the desired properties. HEBM of titanium powder with lampblack using a combination of dry (5 min) and wet (10 min) milling produces Ti/C composite particles (Fig. 1b and Fig. 5a) with an extremely high specific surface area (SSA) - $100 \text{ m}^2/\text{g}$ [19,25]. Notably, after CS the TiC product particles possess essentially the same morphology (Fig. 5b) and have a SSA in a range of $20\text{--}30 \text{ m}^2/\text{g}$.

The Si-C system has relatively low exothermicity ($\text{Si} + \text{C} = \text{SiC} + 73 \text{ kJ/mol}$) and different activation approaches are used in order to produce silicon carbide through self-sustained reactions. HEBM has been applied as an effective tool towards enhancing reactivity [93]. Specifically, it was shown [23] that under the optimal milling conditions sub-micron Si/C composite particles can be prepared (Fig. 6c) in which nano Si grains are embedded within an amorphous carbon matrix. It was also observed that the maximum combustion temperature for the mechanically activated Si/C reactive material is $\sim 1780 \text{ K}$, which is above the melting point of silicon (1687 K). However, comparison of the microstructure of the composite Si/C particles (Fig. 5c) with that of the product SiC powder (Fig. 5d) clearly indicates that their microstructures are almost identical. These examples demonstrate that the hybrid approach of combining CS and HEBM is an effective tool for controlling the microstructure of the ceramic powder products of self-sustained heterogeneous reactions. Recently, this approach was used for obtaining ceramic powders for the $\text{B}_4\text{C-Ti}$ [94] and Ta-Hf-C [95] systems, as well as for producing ultra-high temperature ceramics [96–98].

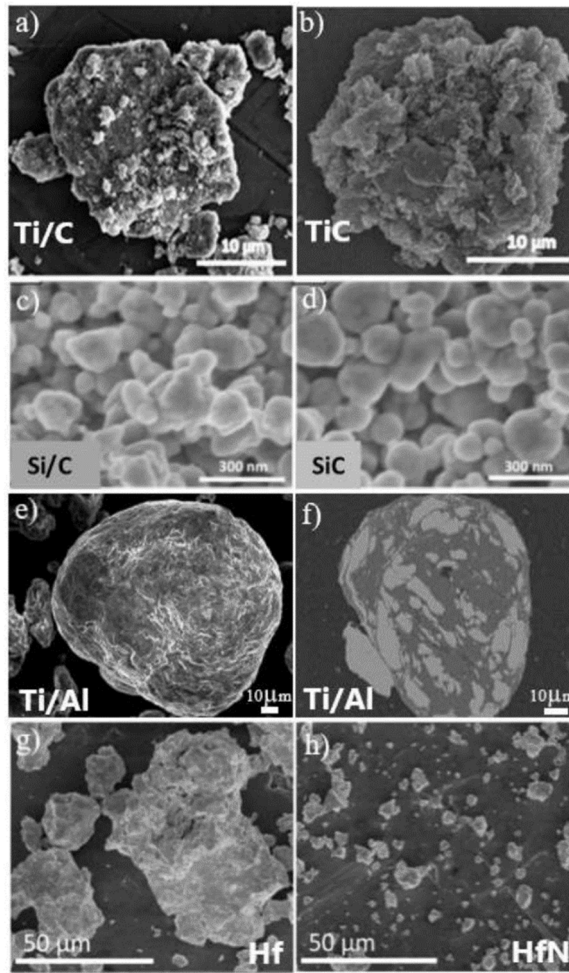


Fig. 5. Typical microstructures of different materials: (a) Ti/C mechanically-induced particle; (b) TiC particle after CS; (c) Si/C mechanically-induced particles; (d) SiC powder after CS; (e,d) Ti/Al mechanically-induced particle; (g) initial Hf powder (h) HfN sub-micron powder.

An additional example that illustrates the effectiveness of HEBM in preparing reactive particles with a desired morphology is related to the manufacturing of spherical particles for 3D-reactive printing applications [99]. It is well known that intensive mechanical treatment often leads to the formation of irregularly-shaped particles [16]. This effect is related to the stochastic motion of grinding balls, which causes brittle components to crack and plastic components to flatten, weld to each other, and harden. The question arises: is it possible to change the motion of the grinding balls to produce additional powder morphologies that are not irregular? As described in Section 2.1, the investigations showed that by varying the operating parameters of the mill, qualitatively different modes for the motion of the ball can be achieved [28]. In recent work [99], the possibility of obtaining essentially spherical reactive composite particles suitable for use in 3D printing technology was demonstrated. Treatment of the initial powders in the Ti-Al system under

the optimum rolling regime, allowed fabrication of Ti/Al reactive composite particles of a desired shape (Fig. 5 e,f).

For all the cases described above, HEBM was carried out up until a critical time, which is the empirically-determined maximum milling time for which reaction had not yet occurred within the milling jar. The treatment was terminated at this critical time and the powder was removed for further processing in a chemical reactor. However, mechanically-induced self-sustained reactions that take place directly in the jars are also of great interest [100]. In our recent work on the mechanochemical synthesis of hafnium nitride powder [101], it was shown that, under intensive mechanical treatment, the conditions for extremely rapid reaction can be achieved. The mechanochemical synthesis of the hafnium nitride powder was carried out in an «Activator 2S» (Activator, Russia) planetary ball mill in a nitrogen atmosphere. Under the optimum conditions, the observed nitridation rates were extremely fast and comparable to those recorded for conventional high temperature processing at 1000 °C. Such high rates are directly related to the microstructural transformation taking place during high-energy ball milling. The proposed mechanism of rapid hafnium nitridation described the continuous formation of a thin product phase layer on the particle surfaces and its subsequent disintegration, which produces fresh metal surfaces that permit additional surface reactions. As a result, a refractory sub-micron hafnium nitride ceramic powder is formed (Fig. 5 g,h).

3.2. *CS and SPS: Rapid synthesis of bulk high-temperature ceramics*

The following reactions were used for one-step fabrication of bulk SiC and B₄C ceramics from reactive mixtures: $\text{Si}+\text{C}=\text{SiC} + 73 \text{ kJ/mol}$ (1) and $4\text{B}+\text{C}=\text{B}_4\text{C} + 71 \text{ kJ/mol}$ (2). Both reactions have relatively low heats of formation with adiabatic combustion temperature of 1600 °C and 682 °C respectively. Prior to sintering, the mixtures of the precursors were subjected to short-term HEBM to produce nanostructured reactive composite particles. This mechanical treatment serves a two-fold purpose for further fabrication of nanostructured bulk ceramics by:

- (a) enhancing the reactivity of the system to: (i) allow reaction initiation well below the melting points of the precursors (~1100 °C for Si-C and 1500 °C for B-C), thus avoiding the influence

of melting on the structural transformations; (ii) permit extremely rapid (20 s for Si-C and ~100 s for B-C) reaction, which completely transforms precursors to the desired ceramic phase; (b) creating a solid-state reactive mixture, which contains precursors mixed at the level of tens to hundreds of nanometers, and that transforms into similarly nano-scale grains of the ceramic product phase during the relatively short sintering time (minutes).

For example, the Si-C mixture during HEBM has been observed to follow a distinct sequence of microstructural transformations [43]. At short milling times (Fig. 6a), the size of the Si particles does not change much, while carbon covers their surfaces. For longer milling times (Fig. 6b), the brittle Si particles experience significant reduction in size, (from microns to sub-micron scale) and their surfaces are covered by carbon. Next, the formation of composite particles is detected, which involves fine Si nano particles covered by an amorphous carbon phase (Fig. 6c). Two hours of HEBM results in the formation of XRD-amorphous nano-composite particles of 100–200 nm in size, which consist of nm-size (5 nm and smaller) Si grains embedded in a carbon matrix (Fig. 6d).

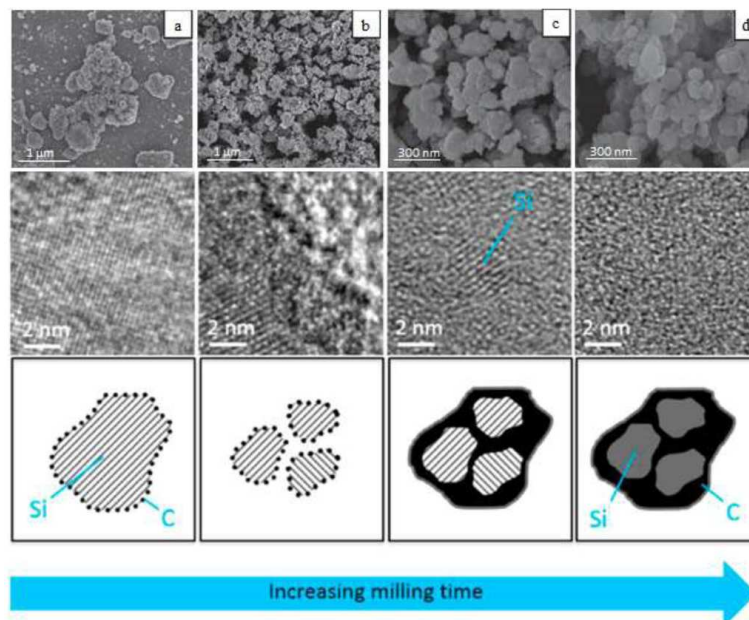


Fig. 6. Sequence of structural transformation during HEBM of Si-C powder mixture.

Similar transformations also occur in the B-C system [44]. Figure 7 illustrates the microstructure of the initial mixture (A) and the composite reactive particles (c-d) produced after 15 min of HEBM. It can be seen that relatively large (10-20 μm) B/C particles consist of boron and carbon with characteristic sizes less than 500 nm.

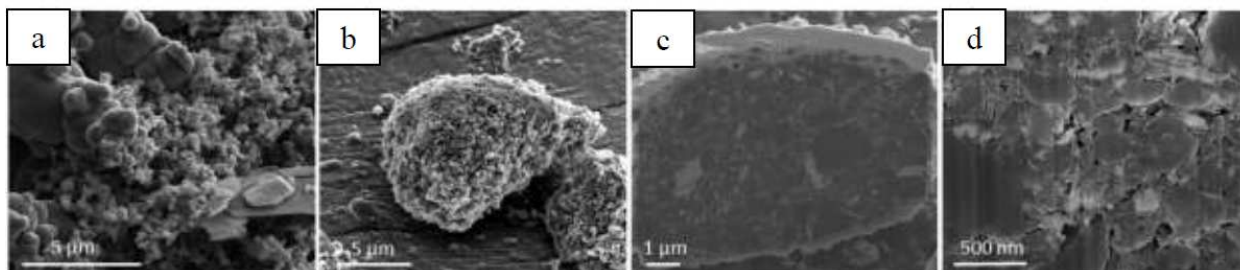


Fig. 7. Microstructures of (a) initial B-C mixture; (b-d) mechanically induced B/C particles.

The prepared powder mixtures were sintered using a conventional SPS regime with a heating rate of 200 $^{\circ}\text{C}/\text{min}$ without any additives. The sintering temperatures were 2000 $^{\circ}\text{C}$ with a dwell time of 10 min and 60 min for Si-C and B-C systems, respectively. It should be noted that for these low exothermicity reactions no significant change of temperature was observed at the reaction initiation points; rather, reaction can only be detected by changes in sample resistivity at ~ 1150 $^{\circ}\text{C}$ for the Si/C mixture and by an increase in gas pressure across the temperature interval 1200 – 1400 $^{\circ}\text{C}$ for the B/C system. However, for highly energetic systems, such as ZrB_2 , TaB_2 , and $\text{B}_4\text{C-TiB}_2$, there was an obvious change in temperature during RSPS [42,102,103].

Electron micrographs of the fractured surfaces from bulk SiC ceramics that were obtained by two-steps (CS followed by SPS) and one-step (RSPS) approaches are shown in Fig. 8. In both cases, the reactive Si/C nanostructured composite powder, obtained after 30 min HEBM of the Si-carbon lampblack mixture was used as a precursor [104]. During conventional SPS of the SiC submicron powder [43], 50 MPa was applied at room temperature and kept constant during the whole process, while for RSPS the pressure (50 MPa) was applied after reaction initiation. It can be seen that SPS ceramics sintered from sub-micron SiC powder possess smaller (0.3 μm) silicon carbide grains (Fig. 8a) than the grain size (~ 5 μm) of the RSPS material (Fig. 8b). This effect can be explained by the higher temperatures in the bulk of the RSPS sample during self-sustained reaction, which leads to substantial grain.

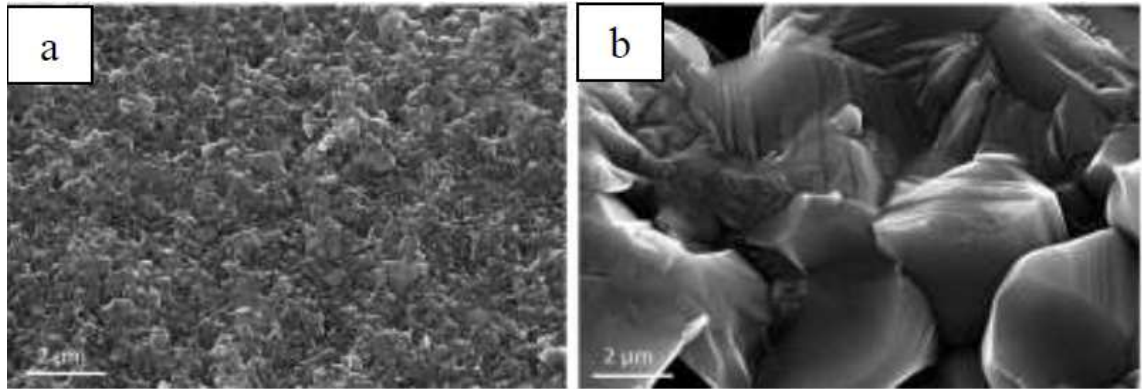


Fig. 8. Typical microstructure of the SiC ceramics obtained by (a) conventional SPS and (b) RSPS.

While the density (3.1 g/cm^3) and micro-hardness ($24 \pm 1 \text{ GPa}$) of both materials were essentially the same, the RSPS ceramic possesses a higher fracture toughness than that for material prepared in two-steps, which were $5.0 \text{ MPa}\cdot\text{m}^{1/2}$ and $4.0 \text{ MPa}\cdot\text{m}^{1/2}$, respectively [104]. It was also shown that the fractured surface of the ceramics produced by conventional SPS of the SiC powder (Fig. 8a) has intergranular features and the sub-micron (200–300 nm) SiC grains can be clearly seen. The fractured surface of the material produced by single-step RSPS (Fig. 8b) has intra-granular features, which suggests that sintering coupled with chemical reaction leads to the formation of stronger necks between the SiC grains. The latter may explain the higher toughness of the RSPS ceramics.

In the case of the B_4C ceramics we demonstrated control over the materials' structure by applying different HEBM times [44]. Typical microstructures of B_4C ceramics prepared by RSPS without any sintering additives are shown in Fig. 9a. It can be seen that the size of the carbide grains varies significantly as a function of milling time. The ceramics obtained by RSPS from the powder subjected to the conventional mixing of the precursors (a) has grain size $\sim 50 \mu\text{m}$, while RSPS of HEBM mixtures for 5min (b) and 15min (c) possess grain size 6 and 3 μm correspondingly. This effect leads to increases in the materials' mechanical properties (Table 1).

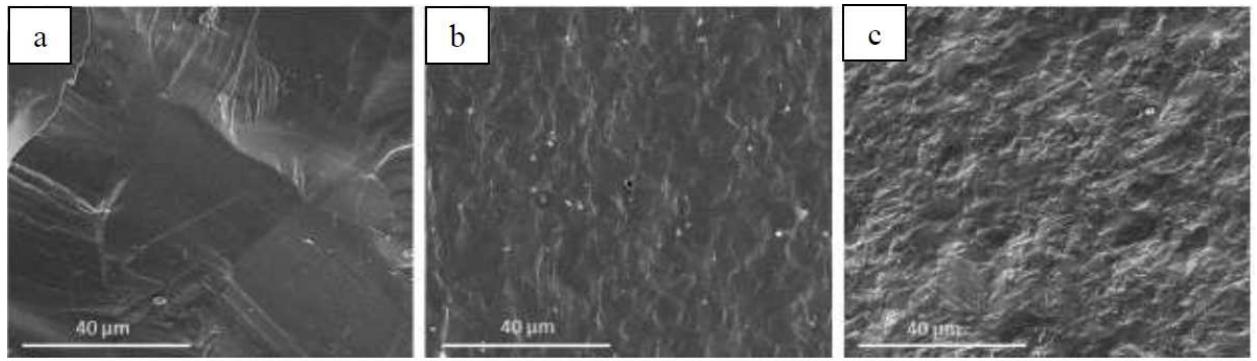


Fig. 9. Typical microstructure of the B₄C ceramics obtained under similar SPS conditions from different B-C mixtures: (a) conventional mixing; (b) 5min of HEBM; (c) 15min of HEBM.

Table 1
Some mechanical properties of the ceramics.

Duration of HEBM (min)	Hardness (GPa)	Fracture toughness (MPa·m ^{1/2})
0	27.0 ± 0.1	3.4 ± 0.1
5	31.6 ± 0.3	3.4 ± 0.2
15	33.3 ± 0.2	4.5 ± 0.2

A similar approach, i.e. RSPS of ceramics from elements, was used in the works of Orru, Cao et al. for fabrication of a variety of high-temperature ceramics, including TaB [42], B₄C-TiB₂ [103], HfB₂ and HfB₂-SiC (whiskers) [105]. Particular attention was paid to the effect of heating rate on the RSPS process [41]. It was demonstrated that in some systems a change in the heating rate leads to a change in the reaction mechanism during the RSPS. Specifically, rapid self-sustained reaction occurs for high heating rates, while a relatively slow solid-phase diffusion reactive sintering mode takes place for lower heating rates.

Sun et al. [106,107] used carbon black and oxides as raw materials. Carbides were formed through carbothermal reduction, then the *in situ* formed intermediate was densified by SPS. Bulk non-porous fine ultra-high temperature HfC, ZrC, and WC ceramics were obtained at a relatively low temperature (up to 1800 °C). The self-sustained reaction between HfSi₂ and carbon was used by Feng et al. [108], to fabricate nanostructured HfC-SiC ceramics, with HfC and SiC grain sizes of 310 and 210 nm, respectively. A similar approach was used by Shahedi et al., [109] to produce a ZrB₂-VB₂-ZrC composite with $HV = 19.2$ GPa and $K_{IC} = 4.5$ MPa·m^{1/2}.

The production of high-entropy ceramics (HEC) has recently generated significant interest [110–112], and includes several borides [113–115] and carbides [116–119]. A HE boride ($\text{Hf}_{0.2}\text{Zr}_{0.2}\text{Ta}_{0.2}\text{Nb}_{0.2}\text{Ti}_{0.2}\text{B}_2$) and a HE carbide ($\text{Hf}_{0.2}\text{Zr}_{0.2}\text{Ta}_{0.2}\text{Nb}_{0.2}\text{Ti}_{0.2}\text{C}$) were also fabricated by flash reactive SPS with a relative density of 99 % and with an observed formation of single phase HEC within 120 s [50].

The examples described above demonstrate that the combination of self-sustained reaction and SPS is a powerful approach for production of various bulk ceramics. It is especially useful for fabrication of high and ultra-high temperature ceramics, which are difficult to sinter by conventional techniques. We also suggest that, in the near future, reactive flash SPS, which combines rapid reactions and rapid densification, has strong potential for synthesis of dense bulk materials.

3.3. *Shock-induced synthesis of ceramics containing metastable c-BN phase*

Shock-induced reaction synthesis (SRS), which involves a combination of a self-sustained, high-temperature (2000–3000 °C) reaction and a shock wave, represents a unique method to produce advanced materials. As mentioned above, there are two fundamentally distinct cases for SRS [120]. In the first case, the shock wave heats the material sufficiently to initiate a reaction, after pressure release that propagates as a deflagration combustion wave with a characteristic reaction time on the order of several milliseconds. In the second case, a gasless reaction takes place directly during the shock wave within several microseconds [68,121]. The latter approach allows the synthesis of a *metastable* phase, which can form only under high-pressure conditions. This synthesis route becomes even more intriguing for solid flame-type reactive systems with an adiabatic combustion temperature (T_{ad}) below the melting points of all precursors, intermediates, and final products. For such systems, solid-state mechanisms of mass transport should govern the reaction process, which at the first glance seems unfeasible.

In our recent works, we have investigated self-propagating reaction in the TiN-3B system in an attempt to fabricate a BN-TiB₂ composite ceramic through the exchange reaction

$\text{TiN}+3\text{B}=\text{BN}+\text{TiB}_2$ [122]. Thermodynamic calculations reveal that this reaction belongs to the family of solid flame systems with an adiabatic combustion temperature equal to 1630 °C, which is lower than the melting points of B (2080 °C), TiN (2930 °C), and TiB_2 (3230 °C), as well as the dissociation temperature of BN (2973 °C). First, it was shown that reaction in this system could not be initiated by thermal or shock wave means after conventional mixing of the powder precursors [26]. Therefore, short-term (45 min) HEBM was used to prepare nanostructured TiN/B composite particles.

XRD performed on the composite powder produced by this intensive mechanical treatment reveals only the TiN phase, indicating that no product phases formed during the HEBM process. Electron micrographs show that the produced powder consists of micron-scale composite particles (Fig. 10a), which consist of nanoscale (5-500 nm) crystallites of B suspended in a fine (10-20 nm) TiN matrix (Fig. 10b). These nanostructured TiN/B composite particles are highly reactive due to the significant increase in interfacial contact area and reduced diffusion distance as a result of the milling process (Fig. 10c). This composite powder was then hand-packed into the innermost of two copper tubes closed with steel caps producing a 50 % TMD pellet. SRS was accomplished following the scheme shown in Fig. 3b, reaching an estimated shock wave pressure of ~15 GPa.

Both XRD and SEM/TEM analysis of the obtained product confirm the formation of c-BN as a result of SRS [122]. Figure 10 d-f shows typical SEM (d, e) and STEM (f) images of a reacted particle. Based on the SEM contrast, one can suggest the presence of four phases in the product material where light phases (B, BN) appeared with darker contrasts, while the phases with higher average atomic mass (TiN, TiB_2) have lighter contrasts. EDS analysis with nanometer spatial resolution in STEM mode (Fig. 10f) confirmed the elemental composition of the phases. Typical HRTEM images of a sample that has been subjected to the shock wave are shown in Fig. 10g. H-BN nano-sheets are present in between the randomly oriented TiB_2 crystallites, while c-BN nano-crystals are primarily observed on the surface of the TiB_2 crystallites (inset of Fig. 10g).

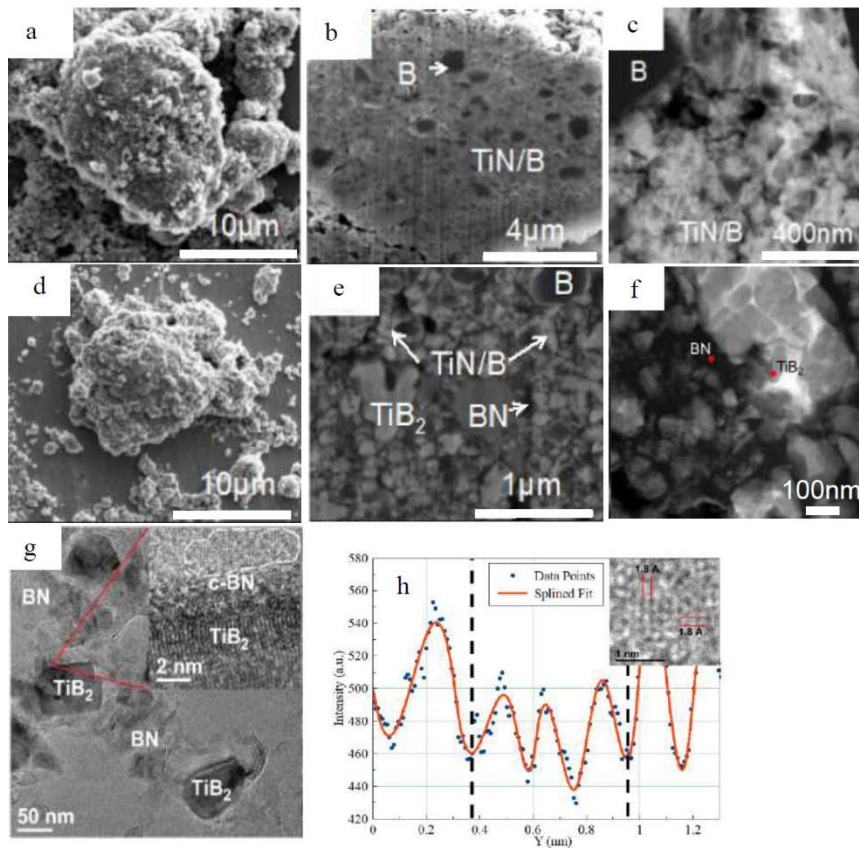


Fig. 10. Microstructures of (a-c) the mechanically induced B/TiN particles; (d-i) SRS products; (g) HRTEM image of the SRS products (h) Intensity distribution on the magnified fragment of the HRTEM image of the c-BN phase.

Figure 10h represents an HRTEM image of a nanocrystal in a low zone crystallographic orientation. The averaged intensity profiles were used to measure the d-spacing in both horizontal (i) and vertical (not shown) directions to increase the signal-to-noise ratio. It was shown that the d-spacing value for the analyzed nano-crystals is equal to 0.183 ± 0.014 nm, which fits within 1% accuracy of 0.181 nm, the (200) d-spacing of the c-BN crystal structure.

These results illustrate that the rapid reactions enabled by high-energy ball milling may occur in the solid state within microseconds with formation of metastable ceramic phases, which can form only at high pressure. Therefore, SRS provides a novel route for the discovery and fabrication of advanced ceramics. The optimization of this technique, defined as obtaining a higher degree of conversion (DoC) to c-BN, can be approached from several engineering directions: (1) through an improved design of experiment to increase the duration of the high pressure period, this assumes that the formation of c-BN is limited by reaction kinetics; (2) through application of

an alternative design of experiment to effectively quench the product material after shock, this assumes that after an initially high degree of conversion, c-BN transitions to h-BN due to high temperatures at low pressure; (3) determination of the reaction initiation mechanism (such as pore collapse, friction between sliding particles, or a shear-induced transition, etc.), as this would permit the selection or preparation of a more reactive initial material.

3.4. Solution combustion synthesis of a metastable metal nitride

Solution combustion-based approaches have attracted attention as a facile, energy-, and cost-effective approach to synthesis of numerous nanoscale materials [12]. Based on the chemical composition of the reactive mixture, it has long been assumed that only oxide ceramics could be produced by this method [11,69]. However, recent breakthroughs in understanding the reaction mechanism suggest otherwise [12]. Those studies revealed that, under certain conditions (typically with excess fuel), the intermediate gaseous combustion products form a reductive gas environment (typically hydrogen-based) that allows reduction of the metal oxide to form metals (Ni, Cu, Co, etc.) or alloys (NiCo, NiCu, etc.) during SCS [13,81,89–91,123]. These promising results suggest that by understanding the fundamentals of combustion in reactive solutions researchers will be able to synthesize a range of compounds including intermetallics, carbides, nitrides and others, which represents a significant broadening of the scope for potential SCS materials.

In our recent work, we have demonstrated for the first time the route that permits direct SCS of a nanoscale metal nitride ceramic (ϵ -Fe₃N) powder, by using reactive gels containing iron nitrate (Fe(NO₃)₃) and hexamethylenetetramine (C₆H₁₂N₄, HMTA) [14]. Nanoscale ϵ -Fe₃N has attracted significant attention due to its structure and unusual magnetic properties [124]. The preparation of single-phase nanoscale ϵ -Fe₃N is challenging. It is known that ϵ -Fe₃N is a metastable phase in every produced form, i.e. bulk, thin film, or nanoparticles [125–127]. The thermodynamic calculations in the considered iron nitrate-HMTA system confirm that Fe₃N does not fit any global minimum of the Gibbs potential in the entire range of investigated conditions.

The temperature–time profiles for the combustion of the gels with different fuel to oxidizer ratios (ϕ) showed that an increase of fuel content leads to a decrease in the maximum combustion temperature, which can be as low as 627 °C. The rate of temperature change within the moving reaction front is in the range of 10^2 – 10^3 °C per second. The reaction duration is in the range of 1.7–2.8 s. Synchrotron x-ray diffraction results, as well as XPS analysis, demonstrated that ϵ -Fe₃N is the only product phase for the combustion of gels with $\phi = 5$. SEM and TEM imaging suggest that all products are large agglomerates that consist of small (5–20 nm) nanoparticles (Fig. 11a). These data imply that the unique conditions within the self-propagating reaction front permit the formation of highly crystalline phases that are far from equilibrium.

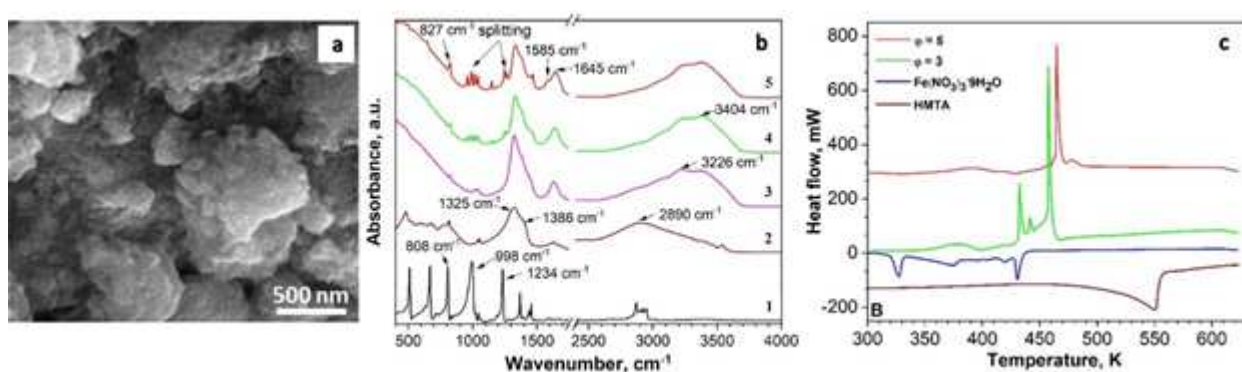


Fig. 11. SEM image of product with $\phi = 5$ (a); FTIR spectra (B) for HMTA (a), and Fe(NO₃)₃·9H₂O (b) as well as reactive gels with $\phi = 1$ (c), $\phi = 3$ (d), and $\phi = 5$ (e); DSC curves (c).

The results from in-situ thermal analysis with mass spectrometry, as well as FTIR analysis of initial reactants and gels allowed us to formulate the mechanism of iron nitride formation in the Fe(NO₃)₃ – C₆H₁₂N₄ system. It was shown that, in the case of fuel rich gels, the formation of an Fe(NO₃)₃ – HMTA coordinated compound takes place during the preparation of the reactive gel. The formation of this coordinated compound was confirmed by the observed splitting of the stretching vibration bands for the C–N bond at 998 and \sim 1234 cm⁻¹ (Fig. 11b) (see also [128]). Thermal analysis (Fig. 11c) for gels with $\phi=5$ shows only one strong exothermic peak with rapid release of multiple gases, including ammonia (NH₃) and hydrocarbons.. This peak corresponds to the thermal decomposition of the Fe(NO₃)₃–HMTA coordinated compound. The presence of

transition metal clusters catalyze further reaction, causing the process rate to increase exponentially. This intramolecular oxidation– reduction reaction between the nitrate oxidizer and the HMTA fuel with the formation of reducing gases and nitrogen directly results in the formation of ϵ -Fe₃N within the combustion wave. This leads to the conclusion that the advantages of self-sustained reactions in gels (short process durations, high reaction temperatures and rapid cooling rates) create unique conditions suitable for one-step formation of metastable ceramics.

SCS was recently also successfully used to produce oxide-carbon precursors for the preparation of Si₃N₄, AlN, TiN, and CrN ceramics [129,130]. Organic residues obtained during the combustion synthesis step significantly accelerated the nitridation in the calcination step. Chu et al. noted that the morphology and sizes of the produced CrN depend on the type of fuel used in the solution combustion stage [130]. They also pointed out that the degree of conversion for Cr₂O₃ to CrN from glycine-derived precursor is found to be higher than that of for alanine, urea, and citric acid.

Nickel sulfide ceramics were synthesized through the solution combustion approach using a mixture of thio-urea fuel as the reducing/sulfidizing agent with glycine fuel as an auxiliary reducing agent [131]. It was shown that the released H₂S gas reduces the decomposition product of NiO to sulfur-containing phases such as Ni₃S₂, NiS and NiS₂ during the combustion reaction. The amount of the different sulfide phases as well as particle size and morphology of the combusted powders are significantly dependent on the type of fuel and the fuel to oxidizer ratio. These works demonstrate that SCS is a novel powerful tool for fabrication of oxygen-free nanoscale ceramics. However, it requires in-depth mechanistic investigation in order to reveal the essential factors that permit formation of nitrides, carbides, sulfides, etc., under SCS conditions.

4. CS: Future directions

Researchers in more than 100 countries are currently using self-sustained reactions for material synthesis. Analysis of the Web of Science database shows that the number of publications on this topic has rapidly increased in recent years, with more than 2600 papers published in 2018.

Several examples of industrial applications of CS are known, including production (40 tons per year) of titanium diboride powders (Hubei DoBo Advanced Ceramics Co., Ltd., China), ferrosilicon nitride (100 tons per year) by NTPF Etalon (Russia), high performance LED phosphors (Ellim Advanced Materials South Ltd., Korea) for LG display, and others.

The approaches briefly described in this review suggest that in the near future new technologies will be added to the repertoire of techniques for industrial scale production of such unique ceramics. The world market on advanced ceramics is continuously growing. While other technologies exist for the production of ceramic powders, it is logical to assume that some novel ceramics will be difficult or essentially impossible to fabricate by such conventional approaches. Taking into account the novel routes to control powder morphology and the flexibility of energy-efficient CS, which is easy to scale up, it may be expected that CS technologies will find their place in the market. The production of sub-micron spherically shaped carbides, borides, carbonitrides, and other ultra-high temperature powders is among the first candidates for such applications.

Combination of CS and SPS for synthesis of monolithic ultra-high temperature bulk ceramics is another promising direction. Indeed, since these compositions possess very high melting points, it is in principle difficult to consolidate the powders to pore-free bulk materials. Recent experiments showed that rapid SC reactions during SPS intensify mass-transport in such systems, and thus enhance their sinterability. Additional investigation is required to optimize this method, but it has substantial potential as a substitute for conventional powder metallurgy approaches used to produce dense, bulk ceramics.

These breakthrough results that demonstrate the ability of CS methods to fabricate metastable compounds are only the first steps in this direction. The near future will show whether or not scientists are able to broaden the list of CS-produced metastable phases and raise the output of products to the laboratory (~kg) scale. If successful, CS may become the go-to method for synthesis of such unique materials.

It is worth noting that self-sustained reactions can also be used for joining materials [132–137]. As previously mentioned, this method should be used when conventional approaches do not work. Such special cases include the joining of refractory materials (high-temperature ceramics) or dissimilar materials where the issue of CTE mismatch is critical. The reported examples of joining carbon-carbon composites [135,136] and silicon carbide to an aluminum alloy [137] demonstrate the effectiveness of CS-based approaches.

Finally, many fundamental questions should be addressed to provide deeper understanding into the phenomenon of self-sustained reaction propagation: (i) Can the majority of such reactions can be accomplished in the solid flame mode, that is essentially through solid-state diffusion?; (ii) What mechanisms might be responsible for the occurrence of solid-state reactions within the microsecond time scale?; (iii) What is the mechanism leading to formation of metastable phases during SCS? (iv) Do SPS conditions influence the kinetics of the self-sustained reactions? In order to answer these and numerous other questions, novel in-situ and operando diagnostics should be designed and built that permit investigation of phenomena with microsecond temporal and nanometer spatial resolutions. These findings will certainly lead to the suggestion of novel synthetic routes applying the CS paradigm.

Acknowledgement

The work was performed with financial support in part from the Ministry of Education and Science of the Russian Federation in the framework of Increase Competitiveness Program of NUST ‘MISiS’ (No. K2-2017-083), implemented by a governmental decree dated March 16, 2013, N 211. J. M. This work was also supported by the Department of Energy, National Nuclear Security Administration, under the Award No. DE-NA0002377 as part of the Predictive Science Academic Alliance Program II.

References

- [1] I.P. Borovinskaya, A.A. Gromov, E.A. Levashov, Y.M. Maksimov, A.S. Mukasyan, A.S. Rogachev, Concise encyclopedia of self-propagating high-temperature synthesis, Elsevier Science, Amsterdam, 2017. doi:10.1016/C2015-0-00439-7.
- [2] A.G. Merzhanov, A.S. Mukasyan, Solid flame (Tverdoplamennoe gorenje), Torus Press, Moscow, 2007.
- [3] A.S. Rogachev, A.S. Mukasyan, Combustion for material synthesis, CRC Press, Boca Raton, Florida, 2014. doi:10.1201/b17842.

- [4] A.L. Bowman, The variation of lattice parameter with carbon content of tantalum carbide, *J. Phys. Chem.* 65 (1961) 1596–1598.
- [5] A.S. Mukasyan, C.E. Shuck, J.M. Pauls, K. V. Manukyan, D.O. Moskovskikh, A.S. Rogachev, The solid flame phenomenon: A novel perspective, *Adv. Eng. Mater.* 20 (2018) 1701065. doi:10.1002/adem.201701065.
- [6] C.E. Shuck, K. V. Manukyan, S. Rouvimov, A.S. Rogachev, A.S. Mukasyan, Solid-flame: experimental validation, *Combust. Flame* 163 (2016) 487–493. doi:10.1016/j.combustflame.2015.10.025.
- [7] E.A. Levashov, A.S. Mukasyan, A.S. Rogachev, D. V. Shtansky, Self-propagating high-temperature synthesis of advanced materials and coatings, *Int. Mater. Rev.* 62 (2017) 203–239. doi:10.1080/09506608.2016.1243291.
- [8] H.H. Nersisyan, J.H. Lee, J.R. Ding, K.S. Kim, K. V. Manukyan, A.S. Mukasyan, Combustion synthesis of zero-, one-, two- and three-dimensional nanostructures: Current trends and future perspectives, *Prog. Energy Combust. Sci.* 63 (2017) 79–118. doi:10.1016/j.peccs.2017.07.002.
- [9] S.T. Aruna, A.S. Mukasyan, Combustion synthesis and nanomaterials, *Curr. Opin. Solid State Mater. Sci.* 12 (2008) 44–50. doi:10.1016/j.cossms.2008.12.002.
- [10] P. Ravindranathan, K.C. Patil, A one-step process for the preparation of γ -Fe₂O₃, *J. Mater. Sci. Lett.* 5 (1986) 221–222. doi:10.1007/BF01672056.
- [11] K.C. Patil, M.S. Hegde, T. Rattan, S.T. Aruna, *Chemistry of nanocrystalline oxide materials*, World scientific, Singapore, 2008. doi:10.1142/6754.
- [12] A. Varma, A.S. Mukasyan, A.S. Rogachev, K. V. Manukyan, Solution combustion synthesis of nanoscale materials, *Chem. Rev.* 116 (2016) 14493–14586. doi:10.1021/acs.chemrev.6b00279.
- [13] K. V. Manukyan, A. Cross, S. Roslyakov, S. Rouvimov, A.S. Rogachev, E.E. Wolf, et al., Solution combustion synthesis of nano-crystalline metallic materials: Mechanistic studies, *J. Phys. Chem. C* 117 (2013) 24417–24427. doi:10.1021/jp408260m.
- [14] A.S. Mukasyan, S. Roslyakov, J.M. Pauls, L.C. Gallington, T. Orlova, X. Liu, et al., Nanoscale metastable σ -Fe₃N ferromagnetic materials by self-sustained reactions, *Inorg. Chem.* 58 (2019) 5583–5592. doi:10.1021/acs.inorgchem.8b03553.
- [15] K. V. Manukyan, Y.S. Chen, S. Rouvimov, P. Li, X. Li, S. Dong, et al., Ultrasmall α -Fe₂O₃ superparamagnetic nanoparticles with high magnetization prepared by template-assisted combustion process, *J. Phys. Chem. C* 118 (2014) 16264–16271. doi:10.1021/jp504733r.
- [16] C. Suryanarayana, Mechanical alloying and milling, *Prog. Mater. Sci.* 46 (2001) 1–184. doi:10.1016/S0079-6425(99)00010-9.
- [17] M. Schoenitz, T. Ward, E.L. Dreizin, Preparation of energetic metastable nano-composite materials by arrested reactive milling, *MRS Proc.* 800 (2003) AA2.6. doi:10.1557/PROC-800-AA2.6.
- [18] M.A. Korchagin, N.Z. Lyakhov, Self-propagating high-temperature synthesis in mechanoactivated compositions, *Russ. J. Phys. Chem. B, Focus Phys.* 2 (2008) 77–82. doi:10.1134/S1990793108010120.
- [19] A.S. Mukasyan, A.S. Rogachev, Combustion synthesis: mechanically induced nanostructured materials, *J. Mater. Sci.* 52 (2017) 11826–11833. doi:10.1007/s10853-017-1075-9.
- [20] A.S. Rogachev, Mechanical activation of heterogeneous exothermic reactions in powder mixtures, *Russ. Chem. Rev.* 88 (2019) 875–900. doi:10.1070/RCR4884.
- [21] G.A. Nersisyan, V.N. Nikogosov, S.L. Kharatyan, A.G. Merzhanov, Chemical transformation mechanism and combustion regimes in the system silicon-carbon-fluoroplastic, *Combust. Explos. Shock Waves.* 27 (1991) 720–724. doi:10.1007/BF00814517.
- [22] Y. Yang, Z.-M. Lin, J.-T. Li, Synthesis of SiC by silicon and carbon combustion in air, *J.*

- Eur. Ceram. Soc. 29 (2009) 175–180. doi:10.1016/J.JEURCERAMSOC.2008.06.013.
- [23] A.S. Mukasyan, Y.-C. Lin, A.S. Rogachev, D.O. Moskovskikh, Direct combustion synthesis of silicon carbide nanopowder from the elements, *J. Am. Ceram. Soc.* 96 (2013) 111–117. doi:10.1111/jace.12107.
- [24] A.S. Rogachev, A.S. Mukasyan, Combustion of heterogeneous nanostructural systems (Review), *Combust. Explos. Shock Waves*. 46 (2010) 243–266. doi:10.1007/s10573-010-0036-2.
- [25] K. V. Manukyan, Y.-C. Lin, S. Rouvimov, P.J. McGinn, A.S. Mukasyan, Microstructure-reactivity relationship of Ti + C reactive nanomaterials, *J. Appl. Phys.* 113 (2013) 024302. doi:10.1063/1.4773475.
- [26] J.M. Pauls, N.F. Shkodich, A.S. Mukasyan, Mechanisms of Self-sustained reaction in mechanically induced nanocomposites: Titanium nitride and boron, *J. Phys. Chem. C*. 123 (2019) 11273–11283. doi:10.1021/acs.jpcc.9b01521.
- [27] A.S. Mukasyan, B.B. Khina, R. V. Reeves, S.F. Son, Mechanical activation and gasless explosion: Nanostructural aspects, *Chem. Eng. J.* 174 (2011) 677–686. doi:10.1016/J.CEJ.2011.09.028.
- [28] A.S. Rogachev, D.O. Moskovskikh, A.A. Nepapushev, T.A. Sviridova, S.G. Vadchenko, S.A. Rogachev, et al., Experimental investigation of milling regimes in planetary ball mill and their influence on structure and reactivity of gasless powder exothermic mixtures, *Powder Technol.* 274 (2015) 44–52. doi:10.1016/j.powtec.2015.01.009.
- [29] E.A. Olevsky, D. V. Dudina, *Field-assisted sintering*, Springer international publishing, Cham, 2018. doi:10.1007/978-3-319-76032-2.
- [30] W. Chen, U. Anselmi-Tamburini, J.E. Garay, J.R. Groza, Z.A. Munir, Fundamental investigations on the spark plasma sintering/synthesis process, *Mater. Sci. Eng. A*. 394 (2005) 132–138. doi:10.1016/j.msea.2004.11.020.
- [31] Z.A. Munir, D. V. Quach, M. Ohyanagi, Electric current activation of sintering: A review of the pulsed electric current sintering process, *J. Am. Ceram. Soc.* 94 (2011) 1–19. doi:10.1111/j.1551-2916.2010.04210.x.
- [32] M. Abedi, D.O. Moskovskikh, A.S. Rogachev, A.S. Mukasyan, Spark plasma sintering of titanium spherical particles, *Metall. Mater. Trans. B*. 47 (2016) 2725–2731. doi:10.1007/s11663-016-0732-8.
- [33] R. Chaim, G. Chevallier, A. Weibel, C. Estournès, Grain growth during spark plasma and flash sintering of ceramic nanoparticles: A review, *J. Mater. Sci.* 53 (2018) 3087–3105. doi:10.1007/s10853-017-1761-7.
- [34] D. Dudina, B. Bokhonov, E. Olevsky, Fabrication of porous materials by spark plasma sintering: A review, *Materials (Basel)*. 12 (2019) 541. doi:10.3390/ma12030541.
- [35] A. Feng, T. Orling, Z.A. Munir, Field-activated pressure-assisted combustion synthesis of polycrystalline Ti₃SiC₂, *J. Mater. Res.* 14 (1999) 925–939. doi:10.1557/JMR.1999.0124.
- [36] Z.A. Munir, The effect of external electric fields on the nature and properties of materials synthesized by self-propagating combustion, *Mater. Sci. Eng. A*. 287 (2000) 125–137. doi:10.1016/S0921-5093(00)00765-6.
- [37] A. Feng, Z.A. Munir, The effect of an electric field on self-sustaining combustion synthesis: Part II. field-assisted synthesis of μ -SiC, *Metall. Mater. Trans. B*. 26 (1995) 587–593. doi:10.1007/BF02653879.
- [38] A. Feng, Z.A. Munir, Field-assisted self-propagating synthesis of β -SiC, *J. Appl. Phys.* 76 (1994) 1927–1928. doi:10.1063/1.357677.
- [39] D. V. Dudina, A.K. Mukherjee, Reactive spark plasma sintering: successes and challenges of nanomaterial synthesis, *J. Nanomater.* 2013 (2013) 1–12. doi:10.1155/2013/625218.
- [40] R. Orrù, G. Cao, Comparison of reactive and non-reactive spark plasma sintering routes for the fabrication of monolithic and composite ultra high temperature ceramics (UHTC) Materials, *Materials (Basel)*. 6 (2013) 1566–1583. doi:10.3390/ma6051566.

- [41] R. Licheri, C. Musa, R. Orrù, G. Cao, Influence of the heating rate on the in situ synthesis and consolidation of ZrB_2 by reactive spark plasma sintering, *J. Eur. Ceram. Soc.* 35 (2015) 1129–1137. doi:10.1016/j.jeurceramsoc.2014.10.039.
- [42] R. Licheri, C. Musa, R. Orrù, G. Cao, D. Sciti, L. Silvestroni, Bulk monolithic zirconium and tantalum diborides by reactive and non-reactive spark plasma sintering, *J. Alloys Compd.* 663 (2016) 351–359. doi:10.1016/j.jallcom.2015.12.096.
- [43] D.O. Moskovskikh, Y. Song, S. Rouvimov, A.S. Rogachev, A.S. Mukasyan, Silicon carbide ceramics: Mechanical activation, combustion and spark plasma sintering, *Ceram. Int.* 42 (2016) 12686–12693. doi:10.1016/j.ceramint.2016.05.018.
- [44] D.O. Moskovskikh, K.A. Paramonov, A.A. Nepapushev, N.F. Shkodich, A.S. Mukasyan, Bulk boron carbide nanostructured ceramics by reactive spark plasma sintering, *Ceram. Int.* 43 (2017) 8190–8194. doi:10.1016/j.ceramint.2017.03.145.
- [45] Q. Song, Z.-H. Zhang, Z.-Y. Hu, S.-P. Yin, H. Wang, Z.-W. Ma, Microstructure and mechanical properties of super-hard B_4C ceramic fabricated by spark plasma sintering with (Ti_3SiC_2+Si) as sintering aid, *Ceram. Int.* 45 (2019) 8790–8797. doi:10.1016/j.ceramint.2019.01.204.
- [46] E. Zapata-Solvas, S. Bonilla, P.R. Wilshaw, R.I. Todd, Preliminary investigation of flash sintering of SiC, *J. Eur. Ceram. Soc.* 33 (2013) 2811–2816. doi:10.1016/j.jeurceramsoc.2013.04.023.
- [47] E.A. Olevsky, S.M. Roling, A.L. Maximenko, Flash (ultra-rapid) spark-plasma sintering of silicon carbide, *Sci. Rep.* 6 (2016) 33408. doi:10.1038/srep33408.
- [48] C. Manière, G. Lee, E.A. Olevsky, All-Materials-inclusive flash spark plasma sintering, *Sci. Rep.* 7 (2017) 15071. doi:10.1038/s41598-017-15365-x.
- [49] S. Grasso, T. Saunders, H. Porwal, B. Milsom, A. Tudball, M. Reece, Flash spark plasma sintering (FSPS) of α and β SiC, *J. Am. Ceram. Soc.* 99 (2016) 1534–1543. doi:10.1111/jace.14158.
- [50] J. Gild, K. Kaufmann, K. Vecchio, J. Luo, Reactive flash spark plasma sintering of high-entropy ultrahigh temperature ceramics, *Scr. Mater.* 170 (2019) 106–110. doi:10.1016/j.scriptamat.2019.05.039.
- [51] R.A. Graham, *Solids under high-pressure shock compression*, Springer New York, New York, NY, 1993. doi:10.1007/978-1-4613-9278-1.
- [52] S.S. Batsanov, *Effects of explosions on materials*, Springer New York, New York, NY, 1994. doi:10.1007/978-1-4757-3969-5.
- [53] V.F. Nesterenko, *Dynamics of heterogeneous materials*, Springer New York, New York, NY, 2001. doi:10.1007/978-1-4757-3524-6.
- [54] L. Davison, *Fundamentals of shock wave propagation in solids*, Springer Berlin Heidelberg, Berlin, Heidelberg, 2008. doi:10.1007/978-3-540-74569-3.
- [55] G.A. Adadurov, I.P. Borovinskaya, Y.A. Gordopolov, A.G. Merzhanov, Technological fundamentals of SHS compacting, *J. Eng. Phys. Thermophys.* 63 (1992) 1075–1081. doi:10.1007/BF00853503.
- [56] L.J. Kecskes, T. Kottke, A. Niiler, Microstructural properties of combustion-synthesized and dynamically consolidated titanium boride and titanium carbide, *J. Am. Ceram. Soc.* 73 (1990) 1274–1282. doi:10.1111/j.1151-2916.1990.tb05191.x.
- [57] H.A. Grebe, A. Advani, N.N. Thadhani, T. Kottke, Combustion synthesis and subsequent, *Metall. Trans. A.* 23 (1992) 2365–2372. doi:10.1007/BF02658038.
- [58] B.H. Rabin, G.E. Korth, R.L. Williamson, Fabrication of titanium carbide-alumina composites by combustion synthesis and subsequent dynamic consolidation, *J. Am. Ceram. Soc.* 73 (1990) 2156–2157. doi:10.1111/j.1151-2916.1990.tb05294.x.
- [59] Y.A. Gordopolov, Formation of graded structures upon shock loading of SHS products, *Mater. Sci. Forum.* 308–311 (1999) 123–127. doi:10.4028/www.scientific.net/MSF.308-311.123.
- [60] S.S. Batsanov, G.E. Blokhina, A.A. Deribas, The effects of explosions on materials, *J.*

- Struct. Chem. 6 (1965) 209–213. doi:10.1007/BF00745942.
- [61] N.N. Thadhani, Shock-induced chemical reactions and synthesis of materials, *Prog. Mater. Sci.* 37 (1993) 117–226. doi:10.1016/0079-6425(93)90002-3.
- [62] S.S. Batsanov, Solid-phase reactions in shock waves: Kinetic studies and mechanism, *Combust. Explos. Shock Waves.* 32 (1996) 102–113. doi:10.1007/BF01992198.
- [63] M.A. Meyers, S.L. Wang, An improved method for shock consolidation of powders, *Acta Metall.* 36 (1988) 925–936. doi:10.1016/0001-6160(88)90147-2.
- [64] N.N. Thadhani, S. Work, R.A. Graham, W.F. Hammett, Shock-induced reaction synthesis (SRS) of nickel aluminides, *J. Mater. Res.* 7 (1992) 1063–1075. doi:10.1557/JMR.1992.1063.
- [65] M.A. Meyers, J.C. La Salvia, L.W. Meyer, D. Hoke, A. Niiler, Reaction synthesis/dynamic compaction of titanium carbide and titanium diboride, *Le J. Phys. IV.* 01 (1991) C3-123-C3-130. doi:10.1051/jp4:1991316.
- [66] K.S. Vecchio, J.C. Lasalvia, M.A. Meyers, G.T. Gray, Microstructural characterization of self-propagating high-temperature synthesis/ dynamically compacted and hot-pressed titanium carbides, *Metall. Trans. A.* 23 (1992) 87–97. doi:10.1007/BF02660856.
- [67] B.W. Asay, B.F. Henson, P.M. Dickson, C.S. Fugard, D.J. Funk, Direct measurement of strain field evolution during dynamic deformation of an energetic material, in: *AIP Conf. Proc.*, AIP, 1998: pp. 567–570. doi:10.1063/1.55702.
- [68] R. V. Reeves, A.S. Mukasyan, S.F. Son, Transition from impact-induced thermal runaway to prompt mechanochemical explosion in nanoscaled Ni/Al reactive systems, *Propellants, Explos. Pyrotech.* 38 (2013) 611–621. doi:10.1002/prop.201200193.
- [69] K.C. Patil, S.T. Aruna, T. Mimani, Combustion synthesis: An update, *Curr. Opin. Solid State Mater. Sci.* 6 (2002) 507–512. doi:10.1016/S1359-0286(02)00123-7.
- [70] P. Erri, J. Nader, A. Varma, Controlling combustion wave propagation for transition metal/alloy/cermet foam synthesis, *Adv. Mater.* 20 (2008) 1243–1245. doi:10.1002/adma.200701365.
- [71] A.S. Mukasyan, P. Dinka, Novel approaches to solution-combustion synthesis of nanomaterials, *Int. J. Self-Propagating High-Temperature Synth.* 16 (2007) 23–35. doi:10.3103/S1061386207010049.
- [72] S. Specchia, G. Ercolino, S. Karimi, C. Italiano, A. Vita, Solution combustion synthesis for preparation of structured catalysts: A mini-review on process intensification for energy applications and pollution control, *Int. J. Self-Propagating High-Temperature Synth.* 26 (2017) 166–186. doi:10.3103/S1061386217030062.
- [73] P. Dinka, A.S. Mukasyan, In situ preparation of oxide-based supported catalysts by solution combustion synthesis, *J. Phys. Chem. B.* 109 (2005) 21627–21633. doi:10.1021/jp054486n.
- [74] A. Cross, S. Roslyakov, K. V. Manukyan, S. Rouvimov, A.S. Rogachev, D. Kovalev, et al., In situ preparation of highly stable Ni-based supported catalysts by solution combustion synthesis, *J. Phys. Chem. C.* 118 (2014) 26191–26198. doi:10.1021/jp508546n.
- [75] A. Vita, G. Cristiano, C. Italiano, S. Specchia, F. Cipiti, V. Specchia, Methane oxy-steam reforming reaction: Performances of Ru/ γ -Al₂O₃ catalysts loaded on structured cordierite monoliths, *Int. J. Hydrogen Energy.* 39 (2014) 18592–18603. doi:10.1016/j.ijhydene.2014.03.114.
- [76] A.S. Mukasyan, P. Dinka, Novel method for synthesis of nano-materials: Combustion of active impregnated layers, *Adv. Eng. Mater.* 9 (2007) 653–657. doi:10.1002/adem.200700076.
- [77] A. Ashok, A. Kumar, R.R. Bhosale, M.A.H. Saleh, L.J.P. Van Den Broeke, Cellulose assisted combustion synthesis of porous Cu-Ni nanopowders, *RSC Adv.* 5 (2015) 28703–28712. doi:10.1039/c5ra03103f.
- [78] B. Lertpanyapornchai, T. Yokoi, C. Ngamcharussrivichai, Citric acid as complexing agent

- in synthesis of mesoporous strontium titanate via neutral-templated self-assembly sol-gel combustion method, *Microporous Mesoporous Mater.* 226 (2016) 505–509. doi:10.1016/j.micromeso.2016.02.020.
- [79] A.A. Voskanyan, K.Y. Chan, Scalable synthesis of three-dimensional meso/macroporous NiO with uniform ultralarge randomly packed mesopores and high catalytic activity for soot oxidation, *ACS Appl. Nano Mater.* 1 (2018) 556–563. doi:10.1021/acsanm.7b00064.
- [80] D.E. Wagner, K.M. Eisenmann, A.L. Nestor-Kalinowski, S.B. Bhaduri, A microwave-assisted solution combustion synthesis to produce europium-doped calcium phosphate nanowhiskers for bioimaging applications, *Acta Biomater.* 9 (2013) 8422–8432. doi:10.1016/j.actbio.2013.05.033.
- [81] A. Khort, K. Podbolotov, R. Serrano-García, Y. Gun'ko, One-step solution combustion synthesis of cobalt nanopowder in air atmosphere: The fuel effect, *Inorg. Chem.* 57 (2018) 1464–1473. doi:10.1021/acs.inorgchem.7b02848.
- [82] S.E. Pratsinis, Flame aerosol synthesis of ceramic powders, *Prog. Energy Combust. Sci.* 24 (1998) 197–219. doi:10.1016/S0360-1285(97)00028-2.
- [83] B. Buesser, S.E. Pratsinis, Design of nanomaterial synthesis by aerosol processes, *Annu. Rev. Chem. Biomol. Eng.* 3 (2012) 103–127. doi:10.1146/annurev-chembioeng-062011-080930.
- [84] X. Yu, J. Smith, N. Zhou, L. Zeng, P. Guo, Y. Xia, et al., Spray-combustion synthesis: Efficient solution route to high-performance oxide transistors, *Proc. Natl. Acad. Sci.* 112 (2015) 3217–3222. doi:10.1073/pnas.1501548112.
- [85] G. V. Trusov, A.B. Tarasov, E.A. Goodilin, A.S. Rogachev, S.I. Roslyakov, S. Rouvimov, et al., Spray solution combustion synthesis of metallic hollow microspheres, *J. Phys. Chem. C.* 120 (2016) 7165–7171. doi:10.1021/acs.jpcc.6b00788.
- [86] G.V. Trusov, A.B. Tarasov, D.O. Moskovskikh, A.S. Rogachev, A.S. Mukasyan, High porous cellular materials by spray solution combustion synthesis and spark plasma sintering, *J. Alloys Compd.* 779 (2019) 557–565. doi:10.1016/j.jallcom.2018.11.250.
- [87] M.G. Kim, M.G. Kanatzidis, A. Facchetti, T.J. Marks, Low-temperature fabrication of high-performance metal oxide thin-film electronics via combustion processing, *Nat. Mater.* 10 (2011) 382–388. doi:10.1038/nmat3011.
- [88] A. Pendashteh, M.S. Rahmanifar, R.B. Kaner, M.F. Mousavi, Facile synthesis of nanostructured CuCo_2O_4 as a novel electrode material for high-rate supercapacitors, *Chem. Commun.* 50 (2014) 1972–1975. doi:10.1039/c3cc48773c.
- [89] K.B. Podbolotov, A.A. Khort, A.B. Tarasov, G.V. Trusov, S.I. Roslyakov, A.S. Mukasyan, Solution combustion synthesis of copper nanopowders: The fuel effect, *Combust. Sci. Technol.* 189 (2017) 1878–1890. doi:10.1080/00102202.2017.1334646.
- [90] A. Kumar, E.E. Wolf, A.S. Mukasyan, Solution combustion synthesis of metal nanopowders: Nickel-reaction pathways, *AIChE J.* 57 (2011) 2207–2214. doi:10.1002/aic.12416.
- [91] A. Kumar, E.E. Wolf, A.S. Mukasyan, Solution combustion synthesis of metal nanopowders: Copper and copper/nickel alloys, *AIChE J.* 57 (2011) 3473–3479. doi:10.1002/aic.12537.
- [92] A.G. Merzhanov, A.S. Rogachev, A.S. Mukas'yan, B.M. Khusid, Macrokinetics of structural transformation during the gasless combustion of a titanium and carbon powder mixture, *Combust. Explos. Shock Waves.* 26 (1990) 92–102. doi:10.1007/BF00742281.
- [93] A.S. Mukasyan, Combustion synthesis of silicon carbide, in: *Prop. Appl. Silicon Carbide*, Gerhardt R, InTech, Vienna, 2011: pp. 389–409. doi:10.5772/15620.
- [94] M.A. Korchagin, A.I. Gavrilov, V.E. Zarko, A.B. Kiskin, Y. V. Iordan, V.I. Trushlyakov, Self-propagating high-temperature synthesis in mechanically activated mixtures of boron carbide and titanium, *Combust. Explos. Shock Waves.* 53 (2017) 669–677. doi:10.1134/S0010508217060077.
- [95] E.I. Patsera, V. V Kurbatkina, E.A. Levashov, A.N. Timofeev, Research into the

- Possibility of producing single-phase tantalum-hafnium carbide by SHS, *Russ. J. Non-Ferrous Met.* 59 (2018) 576–582. doi:10.3103/S1067821218050127.
- [96] S. Vorotilo, A.Y. Potanin, I. V Iatsyuk, E.A. Levashov, SHS of Silicon-based ceramics for the high-temperature applications, *Adv. Eng. Mater.* 20 (2018) 1800200. doi:10.1002/adem.201800200.
- [97] S. Vorotilo, A.Y. Potanin, Y.S. Pogozhev, E.A. Levashov, N.A. Kochetov, D.Y. Kovalev, Self-propagating high-temperature synthesis of advanced ceramics $\text{MoSi}_2\text{-HfB}_2\text{-MoB}$, *Ceram. Int.* 45 (2019) 96–107. doi:10.1016/J.CERAMINT.2018.09.138.
- [98] S. Vorotilo, E.A. Levashov, V.V. Kurbatkina, D.Y. Kovalev, N.A. Kochetov, Self-propagating high-temperature synthesis of nanocomposite ceramics $\text{TaSi}_2\text{-SiC}$ with hierarchical structure and superior properties, *J. Eur. Ceram. Soc.* 38 (2018) 433–443. doi:10.1016/J.JEURCERAMSOC.2017.08.015.
- [99] A.A. Nepapushev, D.O. Moskovskikh, V.S. Buinevich, S.G. Vadchenko, A.S. Rogachev, Production of rounded reactive composite Ti/Al Powders for selective laser melting by high-energy ball milling, *Metall. Mater. Trans. B.* 50 (2019) 1241–1247. doi:10.1007/s11663-019-01553-9.
- [100] L. Takacs, Self-sustaining reactions induced by ball milling, *Prog. Mater. Sci.* 47 (2002) 355–414. doi:10.1016/S0079-6425(01)00002-0.
- [101] A.A. Nepapushev, V.S. Buinevich, L.C. Gallington, J.M. Pauls, T. Orlova, O.M. Miloserdova, et al., Kinetics and mechanism of mechanochemical synthesis of hafnium nitride ceramics in a planetary ball mill, *Ceram. Int.* (2019).
- [102] C. Musa, R. Orrù, R. Licheri, G. Cao, Spark plasma synthesis and densification of TaB_2 by pulsed electric current sintering, *Mater. Lett.* 65 (2011) 3080–3082. doi:10.1016/j.matlet.2011.06.094.
- [103] L. Nikzad, R. Orrù, R. Licheri, G. Cao, Fabrication and Formation mechanism of $\text{B}_4\text{C-TiB}_2$ composite by reactive spark plasma sintering using unmilled and mechanically activated reactants, *J. Am. Ceram. Soc.* 95 (2012) 3463–3471. doi:10.1111/j.1551-2916.2012.05416.x.
- [104] D.O. Moskovskikh, Y.-C. Lin, A.S. Rogachev, P.J. McGinn, A.S. Mukasyan, Spark plasma sintering of SiC powders produced by different combustion synthesis routes, *J. Eur. Ceram. Soc.* 35 (2015) 477–486. doi:10.1016/j.jeurceramsoc.2014.09.014.
- [105] C. Musa, R. Orrù, D. Sciti, L. Silvestroni, G. Cao, Synthesis, consolidation and characterization of monolithic and SiC whiskers reinforced HfB_2 ceramics, *J. Eur. Ceram. Soc.* 33 (2013) 603–614. doi:10.1016/j.jeurceramsoc.2012.10.004.
- [106] S.-K. Sun, G.-J. Zhang, W.-W. Wu, J.-X. Liu, T. Suzuki, Y. Sakka, Reactive spark plasma sintering of ZrC and HfC ceramics with fine microstructures, *Scr. Mater.* 69 (2013) 139–142. doi:10.1016/j.scriptamat.2013.02.017.
- [107] S.-K. Sun, G.-J. Zhang, W.-W. Wu, J.-X. Liu, J. Zou, T. Suzuki, et al., Reactive spark plasma sintering of binderless WC ceramics at 1500 °C, *Int. J. Refract. Met. Hard Mater.* 43 (2014) 42–45. doi:10.1016/j.ijrmhm.2013.10.013.
- [108] L. Feng, S.-H. Lee, H.-L. Wang, H.-S. Lee, Nanostructured HfC-SiC composites prepared by high-energy ball-milling and reactive spark plasma sintering, *J. Eur. Ceram. Soc.* 36 (2016) 235–238. doi:10.1016/j.jeurceramsoc.2015.09.024.
- [109] M. Shahedi Asl, B. Nayebi, Z. Ahmadi, S. Parvizi, M. Shokouhimehr, A novel $\text{ZrB}_2\text{-VB}_2\text{-ZrC}$ composite fabricated by reactive spark plasma sintering, *Mater. Sci. Eng. A.* 731 (2018) 131–139. doi:10.1016/j.msea.2018.06.008.
- [110] D.B. Miracle, O.N. Senkov, A critical review of high entropy alloys and related concepts, *Acta Mater.* 122 (2017) 448–511. doi:10.1016/j.actamat.2016.08.081.
- [111] N.D. Stepanov, N.Y. Yurchenko, S.V. Zherebtsov, M.A. Tikhonovsky, G.A. Salishchev, Aging behavior of the HfNbTaTiZr high entropy alloy, *Mater. Lett.* 211 (2018) 87–90. doi:10.1016/j.matlet.2017.09.094.
- [112] W. Zhang, P.K. Liaw, Y. Zhang, Science and technology in high-entropy alloys, *Sci.*

- China Mater. 61 (2018) 2–22. doi:10.1007/s40843-017-9195-8.
- [113] D. Liu, T. Wen, B. Ye, Y. Chu, Synthesis of superfine high-entropy metal diboride powders, *Scr. Mater.* 167 (2019) 110–114. doi:10.1016/j.scriptamat.2019.03.038.
- [114] J. Gild, Y. Zhang, T. Harrington, S. Jiang, T. Hu, M.C. Quinn, et al., High-entropy metal diborides: a new class of high-entropy materials and a new type of ultrahigh temperature ceramics, *Sci. Rep.* 6 (2016) 37946. doi:10.1038/srep37946.
- [115] G. Tallarita, R. Licheri, S. Garroni, R. Orrù, G. Cao, Novel processing route for the fabrication of bulk high-entropy metal diborides, *Scr. Mater.* 158 (2019) 100–104. doi:10.1016/j.scriptamat.2018.08.039.
- [116] B. Ye, T. Wen, D. Liu, Y. Chu, Oxidation behavior of (Hf_{0.2}Zr_{0.2}Ta_{0.2}Nb_{0.2}Ti_{0.2})C high-entropy ceramics at 1073–1473 K in air, *Corros. Sci.* 153 (2019) 327–332. doi:10.1016/j.corsci.2019.04.001.
- [117] P. Sarker, T. Harrington, C. Toher, C. Oses, M. Samiee, J.-P. Maria, et al., High-entropy high-hardness metal carbides discovered by entropy descriptors, *Nat. Commun.* 9 (2018) 4980. doi:10.1038/s41467-018-07160-7.
- [118] J. Dusza, P. Švec, V. Girman, R. Sedlák, E.G. Castle, T. Csanádi, et al., Microstructure of (Hf-Ta-Zr-Nb)C high-entropy carbide at micro and nano/atomic level, *J. Eur. Ceram. Soc.* 38 (2018) 4303–4307. doi:10.1016/j.jeurceramsoc.2018.05.006.
- [119] E. Castle, T. Csanádi, S. Grasso, J. Dusza, M. Reece, Processing and properties of high-entropy ultra-high temperature carbides, *Sci. Rep.* 8 (2018) 8609. doi:10.1038/s41598-018-26827-1.
- [120] N.N. Thadhani, Shock-induced and shock-assisted solid-state chemical reactions in powder mixtures, *J. Appl. Phys.* 76 (1994) 2129–2138. doi:10.1063/1.357624.
- [121] D. Eakins, N.N. Thadhani, Shock-induced reaction in a flake nickel + spherical aluminum powder mixture, *J. Appl. Phys.* 100 (2006) 113521. doi:10.1063/1.2396797.
- [122] M.T. Beason, J.M. Pauls, I.E. Gunduz, S. Rouvimov, K. V. Manukyan, K. Matouš, et al., Shock-induced reaction synthesis of cubic boron nitride, *Appl. Phys. Lett.* 112 (2018) 171903. doi:10.1063/1.5017836.
- [123] Y. Jiang, S. Yang, Z. Hua, H. Huang, Sol-gel autocombustion synthesis of metals and metal alloys, *Angew. Chemie - Int. Ed.* 48 (2009) 8529–8531. doi:10.1002/anie.200903444.
- [124] R. Niewa, D. Rau, A. Wosylus, K. Meier, M. Wessel, M. Hanfland, et al., High-pressure high-temperature phase transition of γ -Fe₄N, *J. Alloys Compd.* 480 (2009) 76–80. doi:10.1016/j.jallcom.2008.09.178.
- [125] D. Li, Z.D. Zhang, W.F. Li, W.J. Feng, C.J. Choi, B.K. Kim, Electrical and magnetic properties of ϵ -Fe₃N nanoparticles synthesized by chemical vapor condensation process, *J. Magn. Magn. Mater.* 307 (2006) 128–133. doi:10.1016/j.jmmm.2006.03.056.
- [126] Z. Schnepf, A.E. Danks, M.J. Hollamby, B.R. Pauw, C.A. Murray, C.C. Tang, In situ synchrotron X-ray diffraction study of the sol-gel synthesis of Fe₃N and Fe₃C, *Chem. Mater.* 27 (2015) 5094–5099. doi:10.1021/acs.chemmater.5b01811.
- [127] A. García-Márquez, S. Glatzel, A. Kraupner, K. Kiefer, K. Siemensmeyer, C. Giordano, Branch-like iron nitride and carbide magnetic fibres using an electrospinning technique, *Chem. - A Eur. J.* 24 (2018) 4895–4901. doi:10.1002/chem.201705585.
- [128] P. Afanasiev, S. Chouzier, T. Czeri, G. Pilet, C. Pichon, M. Roy, et al., Nickel and cobalt hexamethylenetetramine complexes (NO₃)₂Me(H₂O)₆(HMTA)₂·4H₂O (Me = Co²⁺, Ni²⁺): New molecular precursors for the preparation of metal dispersions, *Inorg. Chem.* 47 (2008) 2303–2311. doi:10.1021/ic7013013.
- [129] A. Chu, M. Qin, X. Jiang, L. Zhang, B. Jia, H. Lu, et al., Preparation of TiN nanopowder by carbothermal reduction of a combustion synthesized precursor, *Mater. Charact.* 81 (2013) 76–84. doi:10.1016/j.matchar.2013.04.010.
- [130] A. Chu, Z. Guo, R. Ud-din, Y. Dong, L. Wang, W. Liu, et al., Effect of fuel type on the aminolysis synthesis of CrN powders from combustion synthesis precursors, *Adv. Powder*

- Technol. 29 (2018) 1439–1444. doi:10.1016/j.appt.2018.03.006.
- [131] N. Ardebilchi Marand, S.M. Masoudpanah, M.S. Bafghi, Solution combustion synthesis of nickel sulfide composite powders, *Ceram. Int.* 44 (2018) 17277–17282. doi:10.1016/j.ceramint.2018.06.188.
- [132] A.S. Mukasyan, J.D.E. White, Combustion joining of refractory materials, *Int. J. Self-Propagating High-Temperature Synth.* 16 (2007) 154–168. doi:10.3103/S1061386207030089.
- [133] T.P. Weihs, Fabrication and characterization of reactive multilayer films and foils, in: *Met. Film. Electron. Opt. Magn. Appl.*, Elsevier, 2014: pp. 160–243. doi:10.1533/9780857096296.1.160.
- [134] J.D.E. White, A.S. Mukasyan, M.L. La Forest, A.H. Simpson, Novel apparatus for joining of carbon-carbon composites, *Rev. Sci. Instrum.* 78 (2007) 015105. doi:10.1063/1.2409861.
- [135] J.D.E. White, A.H. Simpson, A.S. Shteinberg, A.S. Mukasyan, Combustion joining of refractory materials: Carbon–carbon composites, *J. Mater. Res.* 23 (2008) 160–169. doi:10.1557/JMR.2008.0008.
- [136] Y.-C. Lin, A.A. Nepapushev, P.J. McGinn, A.S. Rogachev, A.S. Mukasyan, Combustion joining of carbon/carbon composites by a reactive mixture of titanium and mechanically activated nickel/aluminum powders, *Ceram. Int.* 39 (2013) 7499–7505. doi:10.1016/j.ceramint.2013.02.099.
- [137] Y.-C. Lin, P.J. McGinn, A.S. Mukasyan, High temperature rapid reactive joining of dissimilar materials: Silicon carbide to an aluminum alloy, *J. Eur. Ceram. Soc.* 32 (2012) 3809–3818. doi:10.1016/j.jeurceramsoc.2012.05.002.